Özlem POLAT

THERANOSTIC APPLICATIONS OF GOLD NANOPARTICLES in GENE THERAPY

M.S.
2015

SAMPLE SPINE

FATİH UNIVERSITY

Institute of BioNano Technology

Master in
Bio and Nano Technology Engineering

THERANOSTIC APPLICATIONS OF GOLD NANOPARTICLES in GENE THERAPY

by

Özlem POLAT

January 2015

THERANOSTIC APPLICATIONS OF GOLD NANOPARTICLES in GENE THERAPY

by

Özlem POLAT

A thesis submitted to

BioNano Technology Institute

of

Fatih University

in partial fulfillment of the requirements for the degree of

Master

in

Bio and Nano Technology Engineering

January 2015
Istanbul, Turkey

APPROVAL PAGE

This is to certify that I have read this thesis written by Özlem POLAT and that in my opinion it is fully adequate, in scope and quality, as a thesis for the degree of Master in Bio and Nano Technology Engineering.

_____
Assoc. Prof. Dr. Ramazan ÖZTÜRK
Thesis Supervisor

I certify that this thesis satisfies all the requirements as a thesis for the degree of Master in Bio and Nano Technology Engineering.

_____
Prof. Dr. Ayhan BOZKURT
Head of Department

Examining Committee Members

Assoc. Prof. Dr. Ramazan ÖZTÜRK _____

Assoc. Prof. Dr. Mehmet ŞENEL _____

Assoc. Prof. Dr. Sevim IŞIK _____

It is approved that this thesis has been written in compliance with the formatting rules laid down by the Institute of BioNano Technology.

_____
Prof. Dr. Ayhan BOZKURT
Director

January 2015

THERANOSTIC APPLICATIONS OF GOLD NANOPARTICLES in GENE THERAPY

Ozlem POLAT

M.S. Thesis – Bio and Nano Technology Engineering
January 2015

Thesis Supervisor: Assoc. Prof. Dr. Ramazan OZTURK

ABSTRACT

Gold Nanoparticles (AuNPs) have found increasing applications in medical therapies and diagnostics (theranostics). AuNPs present fascinating attitudes such as their easy synthesis in different types involving materials science, the behavior of the individual particles, size-related electronic, magnetic and optical properties (quantum size effect), and their applications to catalysis and biology. AuNPs have promising aspects to be used in many bioapplications such as drug delivery, imaging, and cancer therapy thanks to their unique optical and chemical properties. In the first part of the study, AuNPs in mainly three shaped; gold nanospheres (AuNS), gold nanocage (AuNC), and gold nanorod (AuNR) were synthesized. They were used in diagnostic application on human breast adenocarcinoma (MCF-7) and human mesenchymal (hMSC) cell lines by antibody surface receptor conjugation and dark-field imaging technique. As a conclusion of diagnostic study, AuNS performed efficiently to enter the cell and AuNC, AuNR were more useful shaped nanoparticles for imaging purposes. In the second part of the study, AuNS was used as siRNA carrying platform in therapeutic application by suppressing the gene (MMP-15) which causes invasion of tumour in cervical carcinoma (HeLa) cell lines. As a result, Reverse Transcription Polymerase Chain Reaction (RT-PCR) analysis and dark-field image showed that poly ethyleneimine (PEI) coated AuNS was successful to carry the siRNA and knockdown the MMP-15 gene expression in HeLa cells.

Keywords: Gold Nanoparticles, SPR, Bioimaging, Gene Delivery, Theranostic

ALTIN NANOPARÇACIKLARIN GEN TEDAVİSİNDEKİ TANI-TEDAVİ UYGULAMALARI

Özlem POLAT

Yüksek Lisans Tezi – Biyo ve Nano Teknoloji Mühendisliği
Ocak 2015

Tez Danışmanı: Doç. Dr. Ramazan ÖZTÜRK

ÖZ

Altın nanoparçacıklar (AuNPs) tıbbi tedavi ve tanı (teranostik) uygulamalarda artarak yer almaktadır. AuNPs malzeme bilimi dahilinde farklı tiplerde sentezlenebilir olma, parçacıkların bireysel davranışlar sergilemesi, boyutlarıyla ilintili olarak elektronik, manyetik ve optik özelliklere sahip olma (kuantum boyut etkisi) ve katalitik, biyolojik uygulamalarda yer alabilme gibi etkileyeci özellikleri ile kendini göstermektedir. AuNPs'ın sahip oldukları benzersiz optik ve kimyasal özellikleri sayesinde ilaç taşınması, görüntüleme ve kanser tedavisi gibi biyolojik uygulamalarda ümit vadedici yaklaşımların olmasını sağlamaktadır. Çalışmanın ilk kısmında, başlıca üç farklı şekile sahip AuNPs; altın nanoküre, altın nanokafes, altın nanoçubuk sentezlenmiştir. Sentezlenen parçacıklar yüzey reseptörü-antikor etkileşmesi ve karanlık alan görüntülenmesi teknikleri kullanılarak insan göğüs adenokarsinoma (MCF-7) ve insan mezenkimal (hMSC) hücre hatlarının teşhis uygulamalarında kullanılmıştır. Teşhis uygulamalarının sonucunda, AuNSin hücre içerisine girebilme eyiliminin diğer parçacıklara gore daha yüksek olduğu ve AuNC, AuNR un ise görüntüleme amaçlı çalışmalarda daha aktif olabilecekleri kanısına varıldı. Çalışmanın ikinci bölümünde, AuNS yumurtalık kanseri hücre hattında (HeLa) tümör yayılmasına sebep olan MMP-15 genenin baskılanması için uygun siRNAyı hücre içine taşımak amacıyla kullanılmıştır. Sonuç olarak, RT-PCR analizi ve dark-field görüntüleme yöntemleri göstermişlerdir ki; poli etilen imin (PEI) kaplı AuNS, siRNA nın HeLa hücrelerine taşınmasında ve MMP-15 geninin susturulmasında başarılı olmuştur.

Anahtar Kelimeler: Altın Nanoparçacıklar, SPR, Biyogörüntüleme, Gen Taşıma, Teranostik

To my parents

ACKNOWLEDGEMENT

I express sincere appreciation to Assoc. Prof. Dr. Ramazan OZTURK. I thank him for his contribution, guidance, patience, experience and support throughout the research and writing of my thesis.

Thanks go to Assoc. Prof. Dr. Sevim ISIK, Res. Assist Aysel KARAGOZ and Res. Assist. Zeynep AYDIN SINIRLIOGLU for their valuable help, suggestions and comments.

I express my thanks and appreciation to my family for their understanding, motivation and patience and the person who encourages me for academic studies, is Res. Assist. Muhammed Rıza AKYUZ. Lastly, but in no sense the least, I am thankful to all colleagues and friends.

TABLE OF CONTENTS

LIST OF TABLES

TABLE

LIST OF FIGURES

FIGURE

LIST OF SYMBOLS AND ABBREVIATIONS

SYMBOL/ABBREVIATION	
Au	Gold
S	Sulphur
AuNPs	Gold Nanoparticles
AuNS	Gold Nanosphere
AgNC	Silver Nanocube
AuNC	Gold Nanocage
AuNR	Gold Nanorod
AuNShell	Gold Nanoshell
DNA	Deoxyribonucleic acid
ssDNA	Single Stranded DNA
RNA	Ribonucleic acid
siRNA	Small interfering RNA
RNAi	Ribonucleic Acid Interference
LSPR	Localized Surface Plasmon Resonance
MCF-7	Breast Adenocarcinoma
hMSC	Human Mesenchymal -Steam Cell-
HeLa	Human Cervical Carcinoma
SERS	Surface Enhanced Raman Spectroscopy
NIR	Near-Infrared Region
CT	Computed Tomography
EGFR	Epithelial Growth Factor Receptor
PEG	Polyethylene Glycol
SH-PEG	Thiolated-Polyethylene Glycol
PVP	Poly (vinyl pyrolidone)
PAA	Polyacrylic Acid
DI	Deionized

UV-vis	Ultraviolent Visible
SEM	Scanning Electron Microscopy
TEM	Transmission Electron Microscopy
PEI	Poly (ethylenimine)
HER2	Growth Factor Receptor 2
DDA	4,4’-dithiodibutyricacid
MMP-15	Matrix Metalloproteinases 15
RT-PCR	Reverse Transcription Polymerase Chain Reaction
GAPDH	Housekeeping gene, internal control
DMEM	Dulbecco’s modified Eagle’s medium
MTT	3-(4,5-dimethylthiazol)-2,5-diphenyltetrazolium bromide
sulfo-NHS	Sulfonated N-Hydroxysuccinimide
CTAB	Cetyltriammonium Bromide
AB	Antibody
MPPs	Matrix Metalloproteinases
RISC	RNA-induced silencing complex
ECM	Extracellular Matrix

INTRODUCTION

1.1 GOLD NANOPARTICLES IN NANOMEDICINE

Although there have been several studies about cancer biology in past two decades, cancer is still the second leading cause of death in all over the world. [1] Diagnosis of cancer in early stages is vital to protect the life of the human by improving the therapeutic strategies in correct time intervals. In this manner, scientists have studied diagnostic and therapeutic development on cancer for decades. In recent years, mostly interested area which promises for early detection of cancer and nontoxic (minimal side effect) therapeutic applications in cancer therapy is nanotechnology. AuNPs can be synthesized in various shapes, sizes, and surface chemistry (see Figure 1.1) which are vital for usage of AuNPs in drug delivery systems and as therapeutic agents due to their unique chemical and physical properties. [2] Specific targeting of desired biologically active components such as drug, protein, gene, etc. by gold nanoparticles (AuNPs) to cancer cells and photothermal and gene therapy methods with AuNPs are attractive tools for cancer treatments (see Figure 1.2). [3]

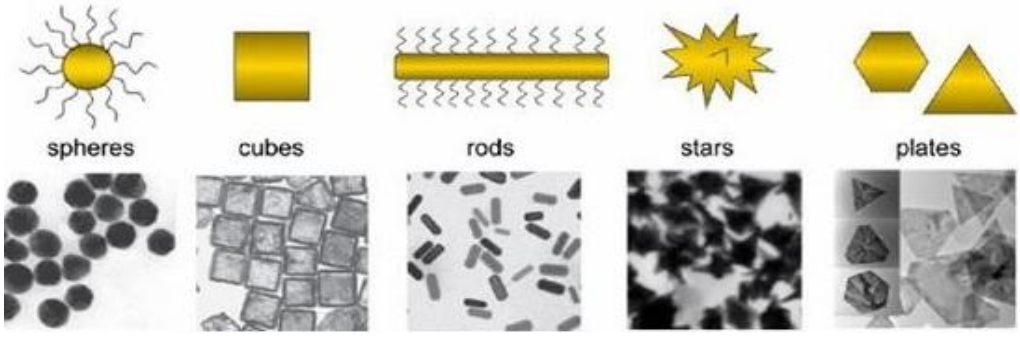

Figure 1.1 Examples of different AuNPs. [4, 5]

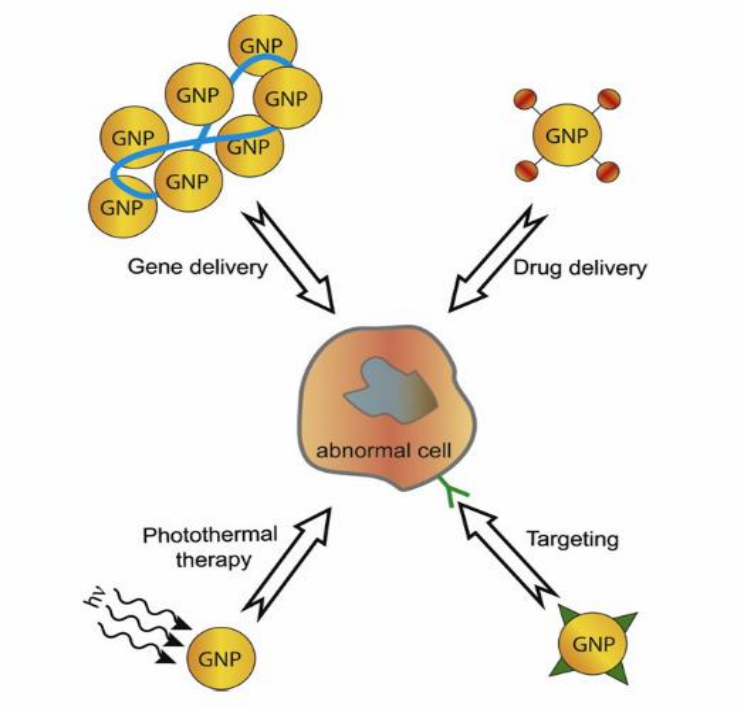

Figure 1.2 Various applications of AuNPs in cancer treatments. [6]

1.2 PHYSICAL AND CHEMICAL PROPERTIES of AuNPs

Gold colloids have fascinated scientists for over a century and are now heavily utilized in chemistry, biology, engineering, and medicine. AuNPs are mostly used plasmonic nanoparticles in several applications in nanotechnology due to their inherent chemical, electrical, and optic characteristics which can be explained with quantum mechanics. [7, 8]

Optical behaviors of AuNPs changes in nanoscale across the bulk; it starts to absorb light in single wavelength. This phenomenon is described with Localized Surface Plasmon Resonance (LSPR) which is the coherent excitation of all the “free” electrons within the conduction band, leading to an in-phase oscillation. [9]

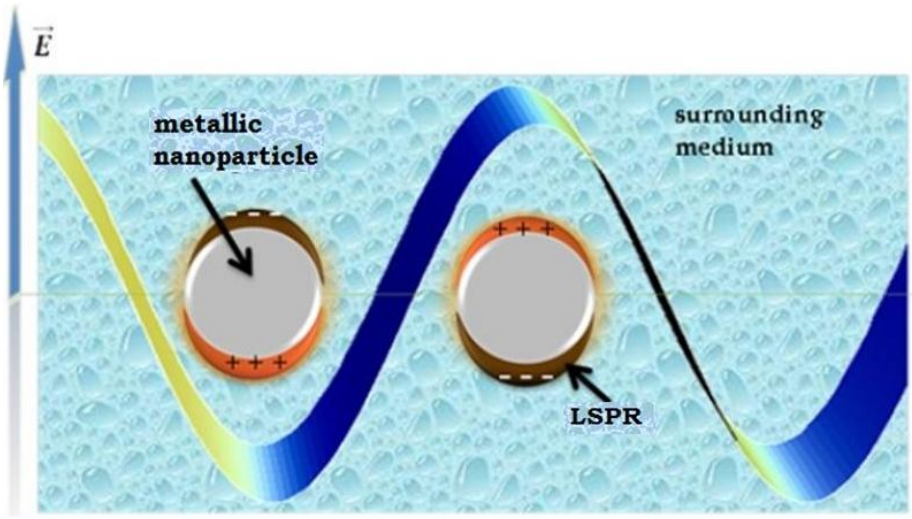

Figure 1.3 Schematic of the electron charge displacement (valence electrons) in a metallic NP (LSPR) interacting with an incident plane wave, with electric field polarized E into a host matrix. [10]

The optical properties of AuNPs change when particles aggregate and the conduction electrons near each particle surface become delocalized and are shared amongst neighboring particles/molecules. When this occurs, the surface plasmon resonance shifts to lower energies, causing the absorption and scattering peaks to bathochromatic shift (red-shift) to longer wavelengths, by using this attitude of AuNP, they are used in many sensor applications in biology. [11, 12] The composition (size, shape, etc.) of the AuNP influences the LSPR properties (see Figure 1.3) which indicates the morphological clues about the synthesized particles. When the size and shape of the particle change the LSPR also shifts where the absorption energy of the particle localized.

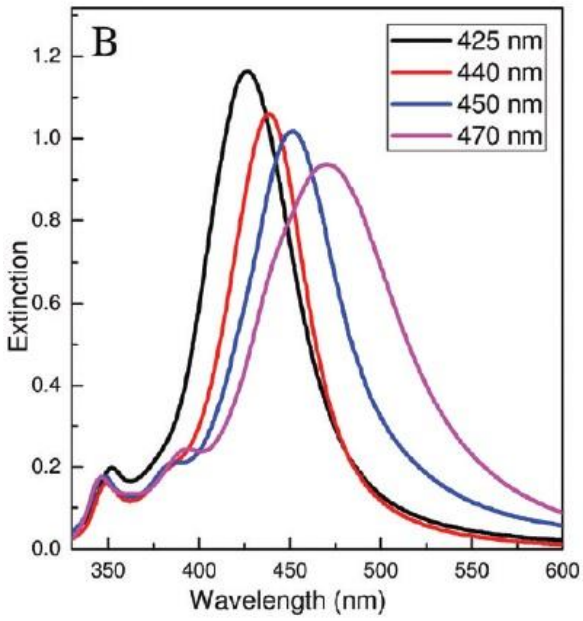

Figure 1.4 SPR of silver nanocubes (AgNCs) with a size of 25, 39, 52, and 86 nm. [13]

There are numerous fabrication methods for AuNPs; the simplest one is the synthesis which is based on reduction of gold salt with proper reducing agent and surfactants which is used to prevent aggregation during the synthesis process. In the synthesis process of AuNPs, the size and shape can be tuned by changing some reaction parameters such as concentration of used metal (gold) salt, reducing agent, temperature. [14] AuNPs with organic monolayer, acts as a barrier between the nanoparticle core and the environment, and effectively protects and stabilizes the core integrity, which is fundamentally important in modifying the interactions of the nanoparticle with its environment, takes important role in delivery systems to combine the target molecule to the surface of the particle by thiol-gold conjugation or electrostatic interaction. [15, 16] Due to chemical modification available surface structure of AuNP, they can be used easily in biological systems with biocompatible surface ligand conjugations and they are favorable in several bioapplications such as sensing, imaging, drug delivery and therapy. [17] To sum up, AuNPs are attractive materials with their unique physical and chemical properties which allow for preparing of the particles in desired size, shape and morphology with essential surface modification.

1.3 AuNPs in BIOLOGICAL APPLICATIONS

In recent years, the use of nanoparticles, particularly metal nanoparticles has expanded in biomedical research. They are used in diagnosis and therapeutics due to their unique properties of small size, large surface area to volume ratio, high reactivity to the living cells, stability over high temperatures and translocation into the cells, etc. Especially, AuNPs are promising nanoparticles which are inert and relatively less cytotoxic and extensively used for various applications including drug and gene delivery because of their versatility and multifunctionality. [18-20] AuNPs can be functionalized to be able to use in biological applications (see Table 1.1).

Table 1.1 Summary of common AuNP functionalization methods and their applications. [21]

Functional Group	**Ligands/Carrier Molecule**	**Key Feature**	**Application**	**Reference**
Polyethylene Glycol (PEG)	PEG with ligands such as a dye attached through thiol group	Adherence to the cell membrane	Cellular and intracellular targeting, biodistribution studies	[22, 23]
Amine Group	PEG	siRNA (small interference RNA) carrier	Useful in RNAi (RNA interference) technology	[24]
Carboxyl Group	Proteins	-	Various depending on the protein	[25]
Peptide	Cell surface receptors, amyloid inhibitory peptide + sweet arrow peptide, antibody, octrotide peptide	Cytoplasmic and nuclear translocation, adjuvant, targeting carcinoma cells analogue of somatostatin	Cellular and intracellular targeting, macrophage and pro-inflammatory cytokine elicitation bioimaging imaging of cancer cells	[26-28]

Table 1.1 (cont.)

DNA	Aptamer, PEGylated gold poly (β-amino ester), Thiolated ssDNA (single stranded DNA) of RNA I gene, antisense DNA oligonucleotides	Targeting Prostate cancer cells , siRNA carrier, binds to antisense RNA of p53	Bioimaging, gene delivery rnai-regulation of transgene expression, detection of specific genes e.g., for microbial detection	[29, 30]
RNA	Polyvalent RNA-gold nanoconjugates	-	RNAi	[31, 32]
Antibodies	scFv Antibodies against various pathogens	Smaller size, label fidelity	Immunoassays treatment and diagnosis e.g., antibodies against aflatoxins	[32]

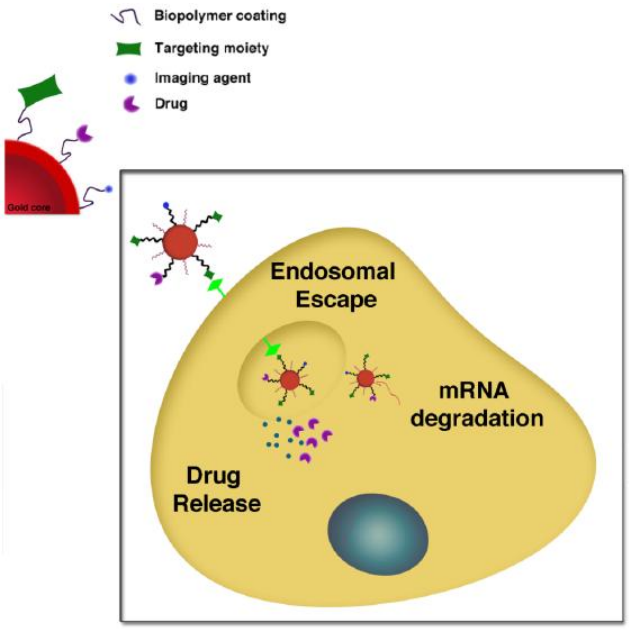

Figure 1.5 Multifunctional NP-based systems for tumor targeting, delivery and imaging. [33]

AuNPs surface is available for several types of ligands such as polyethylene glycol (PEG) molecules, nucleic acids (DNA and RNA), peptides, antibodies, and also small drug molecules conjugation via covalently with Au-S bonding or electrostatic.

1.3.1 Bioimaging

AuNPs can be functionalized with thiolated biomolecules or synthetic polymers which let the particles to be soluble in water or organic solvents and gain biocompatibility. For example; AuNPs which have been biocompatible by surface modification method with SH-PEG, have been reviewed as a contrast agent for tumor vascular agents. Early stage diagnosis of numerous types of cancers are difficult by using available techniques, however AuNPs can be used as diagnostic agents at an early stage of onset for oral squamous epithelial cells. [34] AuNPs can also be conjugated with antibodies which are specific to cancer-associated proteins have been used to image cancerous cells. In one example, AuNP conjugates with antibodies to epithelial growth factor receptor (EGFR) were incubated with oral epithelial cancerous and noncancerous epithelial cells. Light microscopy experiments show that conjugates bind to cancer-ous cells with a six times greater affinity than the non-cancerous controls, thus making this technique potentially useful for the detection of cancer cells. [35] Studies based on imaging of tumors have been focused on nanoparticles functionalized with fluorophores, peptides, cell adhesion molecules, aptamers or other biomolecules to target specific tissues. [36]

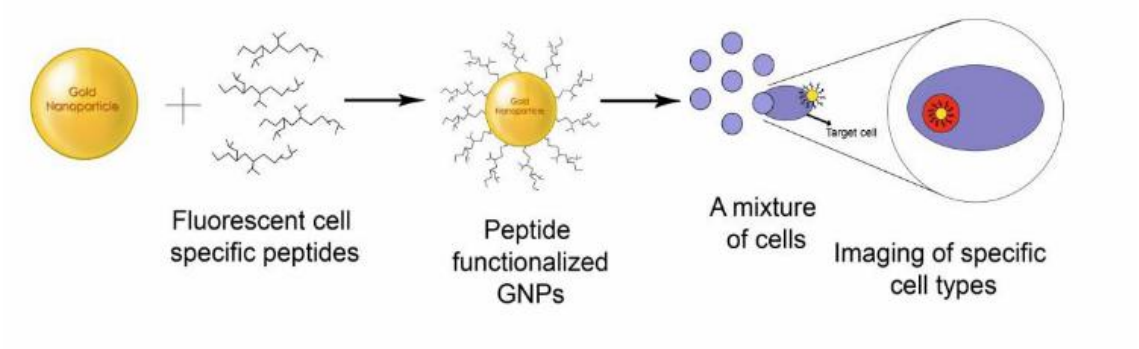

Figure 1.6 AuNPs functionalized with cell specific peptides for bioimaging. [21]

For X-Ray based imaging techniques such as computed tomography (CT) conventional iodine-based contrast agents are currently used in the clinic because of

iodine's high X-Ray absorption, however usage of iodine based agents has several limitations, including short imaging times due to rapid renal clearance, renal toxicity, and vascular permeation. [37] Au (gold) which has a higher X-ray absorption coefficient than iodine (5.16 and 1.94 cm^2/g, respectively, at 100 keV), overcomes these limitations. [38] Therefore, AuNPs have advantages to use as CT imaging contrast agent. [39]

In Fluorescence imaging, AuNPs especially, AuNR and AuNShell (Gold Nanoshell) which have LSPR at around NIR (Near Infrared) window (650−900 nm) which let the particles to behave like a fluorescence particle, can be used in biological imaging techniques. [40]

Surface enhanced Raman Spectroscopy (SERS) imaging is another technique which is widely used in biological, based on molecular vibrations and rotations. By using Raman Spectroscopy, details about the molecules can be analyzed but it has some limitation because of its low sensitivity, since only one photon in 10^8 is Raman scattered. Absorption upon AuNPs surfaces enhances the intensity of the vibrational spectra of Raman active molecules by several orders of magnitude. [41]

Optical imaging by plasmonic AuNPs which have extraordinary light scattering properties get various when the size and shape change is very useful technique in biological imaging. AuNPs are non-photobleaching and tunable nanomaterials compared to fluorescence dyes, they have more life time during the imaging. These properties have encouraged investigations of AuNPs as contrast agents for light scattering imaging. For example, El Sayed et al. worked on differentiation of cancerous cells from healthy cells by using light scattering AuNPs which were conjugated with surface specific receptor of nonmalignant epithelial cell line with dark-field microscopy. [35]

1.3.2 Drug Delivery

In drug delivery, AuNPs are attractive building blocks for efficient and controllable drug delivery systems. [42] Because they exhibit low cytotoxicity and good cell permeability and offer high drug-loading efficacy due to their high surface area to volume ratio stemming from their nanometric size. In addition, AuNPs have been used

for the co-administration of protein drugs due to their ability to cross cellular membranes, possibly due to the interaction of GNPs with cell surface lipids. [43] Moreover, AuNPs can be synthesizing easily in different shapes and sizes which give different light scattering properties to them. For the designing of uploading systems of drug in the target cell, tunable physical properties and available surface modifications of AuNPs are very important for smart drug delivery systems. For instance, Xia et al. worked on gold nanocages which were encapsulated with a thermal-responsive polymer. On exposure to a near-infrared laser, the light is absorbed by the nanocage and converted into heat, triggering the collapse of the polymer. Thus, the pre-loaded effectors can escape from the nanocage. When the laser is turned off, the polymer chains will relax back to the extended conformation and terminate the release (see Figure 1.7).

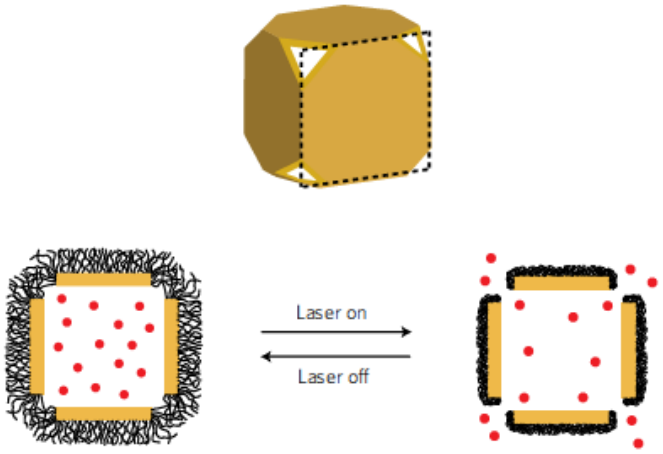

Figure 1.7 Schematic illustration for the controlled release system. [44]

1.3.3 Gene Delivery

Gene delivery is another therapeutic application where AuNPs are being explored for their potential. AuNPs can be modified and synthesized in suitable conditions to encapsulation and releasing of the target gene in the cancer cell. In gene

therapy, one of the methods is ribonucleic acid interference (RNAi) technology which uses synthetic small interference RNAs (siRNA), is unstable in physiological conditions and has low cellular uptake ability due to its high molecular weight and negatively charged structure into the target cancerous cell. Therefore transfer of biomolecules (RNA, ssDNA, siRNA) into the target cancerous cells in efficient way and by making the endosomal escape of the cargoes possible is very important to activate the purpose which may be silence or express the gene signal in cytoplasm. [45] siRNA can be conjugated to the AuNP by two different approaches; (1) Covalent approach: by using gold-thiol binding affinity, thiolated siRNA is used to conjugate with the nanoparticle; (2) Ionic approach: negatively charged siRNA has interaction with surface modified AuNP by positively charged polymer/polypeptide through ionic interactions.

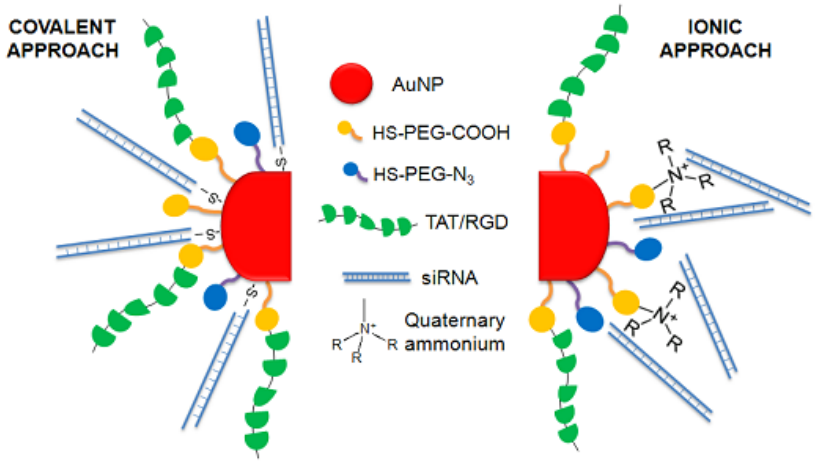

Figure 1.8 Multifunctional siRNA-gold nanoparticles with several biomolecules. [46]

In an example, Giljohann et al. [47] conjugated the siRNA to the gold surface of the nanoparticle via thiol groups to increase transfer efficiency, while Lee et al. [48] studied siRNA-AuNS-PEG conjugation to decrease the biodegradation of the siRNA. Furthermore, Wang et al. [49] chose poly (ethylenimine) (PEI) as both reducing and capping agent via nitrogen to the AuNS surface to carry the siRNA molecule.

1.3.4 Photothermal Therapy

AuNPs are used as photothermal therapy agents, especially in cancer applications, thanks to their high photon absorption which get various when the size and shape of the particle versatile. AuNR and AuNShell are some examples of AuNPs which convert the photon energy to thermal energy when they are irradiated with correct wavelength because of their LSPR in near infrared region. Released heat destroys the attached cancer cells by antibody conjugation on the AuNPs. For example, nanoshells conjugated to anti- bodies against human epidermal growth factor receptor 2 (HER2) were incubated with cancerous cells over-expressing HER2 receptors. These cells were then irradiated with near- IR light at a frequency that is resonant with the surface plasmon resonance of the nanoshell. Light absorption leads to heating, which causes cell death. [50]

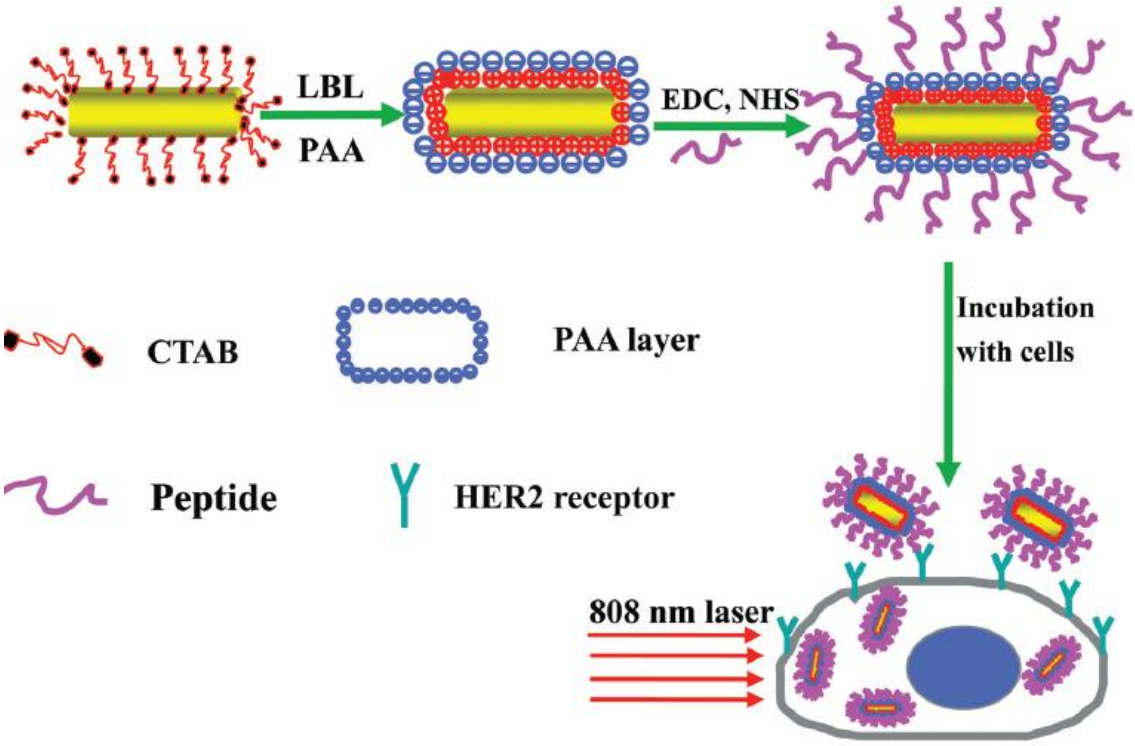

Figure 1.9 Scheme showing process involved in the synthesis of targeted peptide functionalized gold nanorods with polyacrylic acid (PAA) modification and the selective photothermal therapy. [51]

CHAPTER 2

EXPERIMENTAL PROCEDURES

2.1 DIAGNOSTIC STUDY WITH AuNPs

AuNPs were used as diagnostic agents to detect the breast cancer by using antibody-surface receptor conjugation with nanoparticle vectors. Three different shaped and sized AuNPs which were gold nanosphere (AuNS), gold nanocage (AuNC), and gold nanorod (AuNR) were synthesized and modified as biocompatible and antibody conjugated vectors to monitor the MCF-7 and hMSC cell lines by dark-field scattering microscopy.

2.1.1 Materials

The hydrogen tetrachloroaurate ($HAuCl_4$), cetyltrimethylammonium bromide (CTAB), ascorbic acid, silver nitrate ($AgNO_3$, 99%), sodium borohydride ($NaBH_4$), ethylene glycol (EG), poly (vinyl pyrolidone) (PVP, Mn ≈ 55 000), and 4,4'-dithiodibutyricacid (DDA), sulfo-NHS were obtained from Sigma-Aldrich, Germany. EDC.HCl and sodium sulfide (Na_2S, 99%) were purchased from Alfa Aesar, Germany. Sodium citrate dihydrate ($C_6H_5Na_3O_7.2H_2O$) (SAFC, Austria), PEG-SH (poly (ethylene glycol) thiol) (Laysan Bio, Inc) were purchased. All aqueous solutions were prepared with deionized (DI) water (18.2 MΩ.cm @ 25°C).

2.1.2 Synthesis and Characterization of AuNPs

2.1.2.1 Gold Nanosphere (AuNS)

In the synthesis procedure of AuNS, 20 mL 1mM $HAuCl_4$ solution was prepared and boiled at 100^{o}C with continuous stirring for 15 min. Next, 2 mL 1% citrate solution was added into the solution quickly. The solution color changed from yellow to dark purple and then red indicating the formation of nanoparticle. SPR absorbance of the

nanoparticle was measured by Ultraviolent-visible (UV-vis) Spectrophotometer and particle size was analyzed by Scanning Electron Microscopy (SEM).

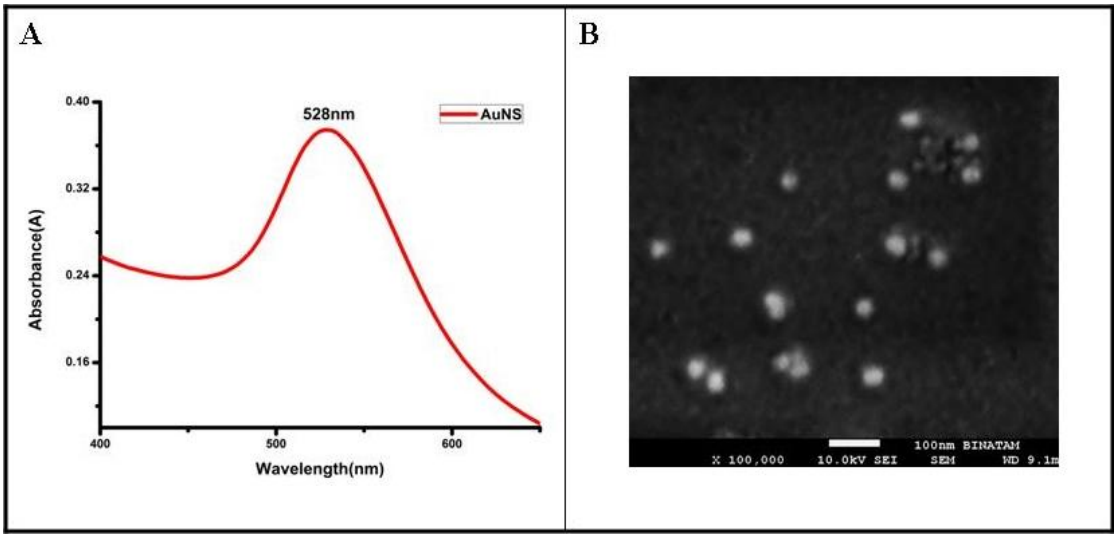

Figure 2.1 UV-vis spectra of AuNS with absorption maxima at 528 nm (a), SEM image of AuNS~40 nm (b).

2.1.2.2 Silver Nanocube (AgNC) Template

For AgNC synthesis, polyol synthesis method was followed according to [52]. Briefly, 35 mL of anhydrous Ethylene glycol (EG) was heated to 140 ^{o}C in oil bath for 1 hour with continuous stirring at 400 rpm. 0.2g of poly (vinyl pyrolidine) (PVP~55 000) was dissolved in 10 mL EG and added to the hot EG solution. Then, the temperature was set to 150^{o}C. One hour ago, Na_2S was weighted 0.0072g and dissolved in 10 mL EG. After PVP had been added, 0.4 mL of Na_2S solution was added to the heating EG solution. Then 0.24g of $AgNO_3$ was dissolved in 5 mL EG freshly, and 3 mL of that solution was added slowly into EG solution and stirring rate was decreased to 100 rpm. The color of the solution became brown. When the color became transparent, the stirring was stopped. After 20 min, stirring was set to 400 rpm again and stirred until the solution became nontransparent. To clean the AgNCs from the solvent and the extra PVP; the solution was diluted with DI water and centrifuged at 13000 rpm for 10 min. The settled part of the colloid was re-suspended in 20 mL DI water.

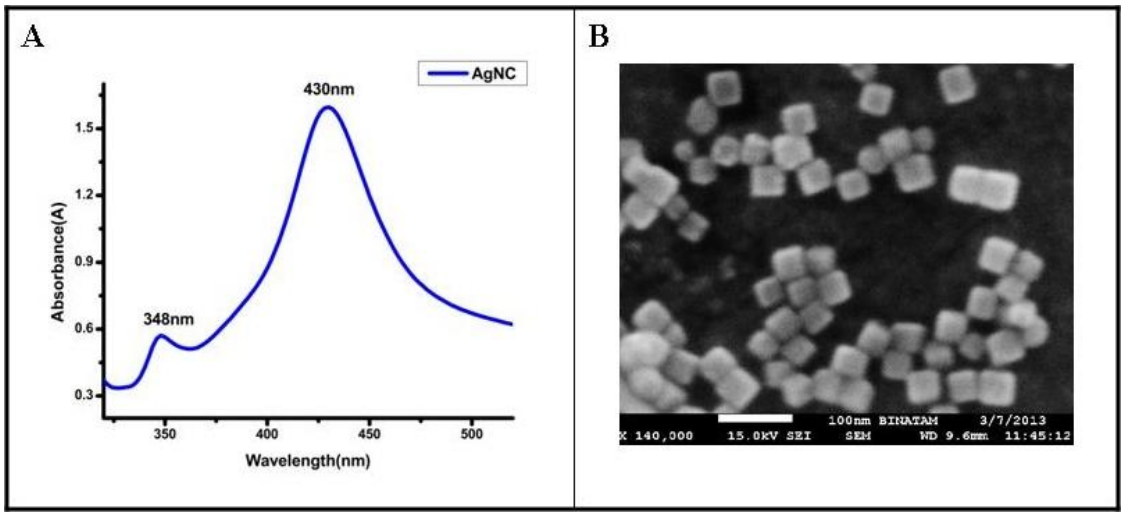

Figure 2.2 UV-vis spectra of AgNC with absorption maxima at 430 nm (a), SEM image of AgNC~50 nm (b).

2.1.2.3 Gold Nanocage (AuNC)

AuNCs were synthesized according to the study [53]. Briefly, 20 mL of previously prepared silver nanocube template (~40 nm) was first cleaned and heated up to boiling with stirring rate of 300 rpm. $HAuCl_4$ solution (0.1g/ L) was injected slowly until the SPR spectrum peak of the solution shifted to 600 nm. The AuNCs solutions were then continuously refluxed until their absorption spectrum became stable and the solution was then cooled down to room temperature. The solution was kept at room temperature overnight and AgCl was filtered off from the solution.

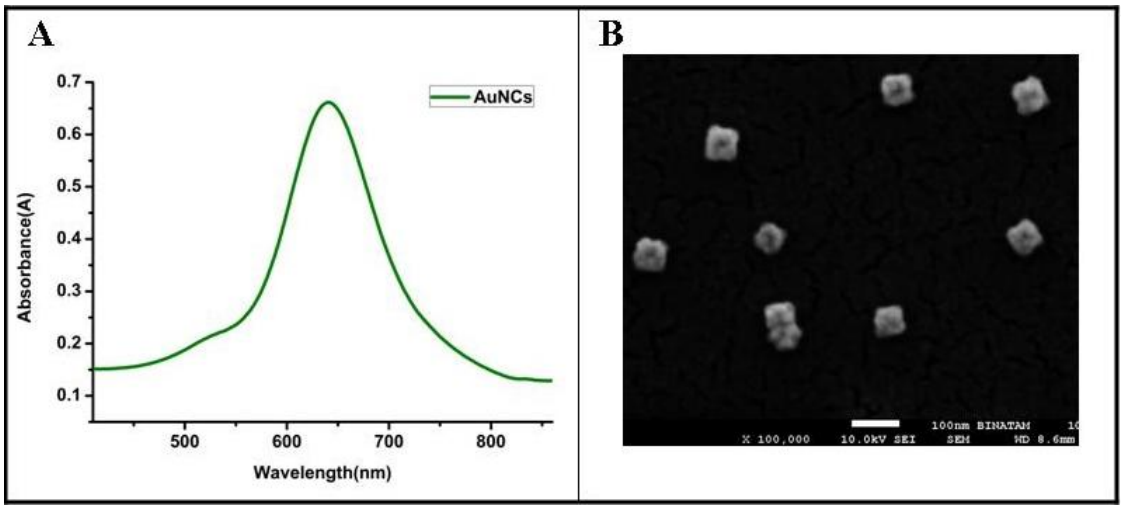

Figure 2.3 UV-vis spectra of AuNC with absorption maxima at 640 nm (a), SEM image of AuNC~60 nm (b).

2.1.2.4 Gold Nanorod (AuNR)

AuNR was synthesized by seed mediated method according to the literature [54]. Seed solution was prepared by using 10 mL of 0.2M CTAB and 5mL 0.001M $HAuCl_4$ solutions, and adding 0.6 mL of ice-cold 0.01M $NaBH_4$ with continuous stirring at 30^{o}C. Growth solution was prepared with 100 mL of 0.2M CTAB and 100 mL of 0.001M $HAuCl_4$ solutions by stirring at 30^{o}C. Next, 4.5 mL of 0.004M of $AgNO_3$ was added and stirring was stopped and 1.4 mL of 0.0788M ascorbic acid was added at room temperature without disturbing. When the color of the solution became colorless completely, 160 µL of seed solution was added to the growth solution. The solution was remained overnight. Finally, the excess CTAB was cleaned twice by centrifugation at 14000 rpm for 15 min with DI water.

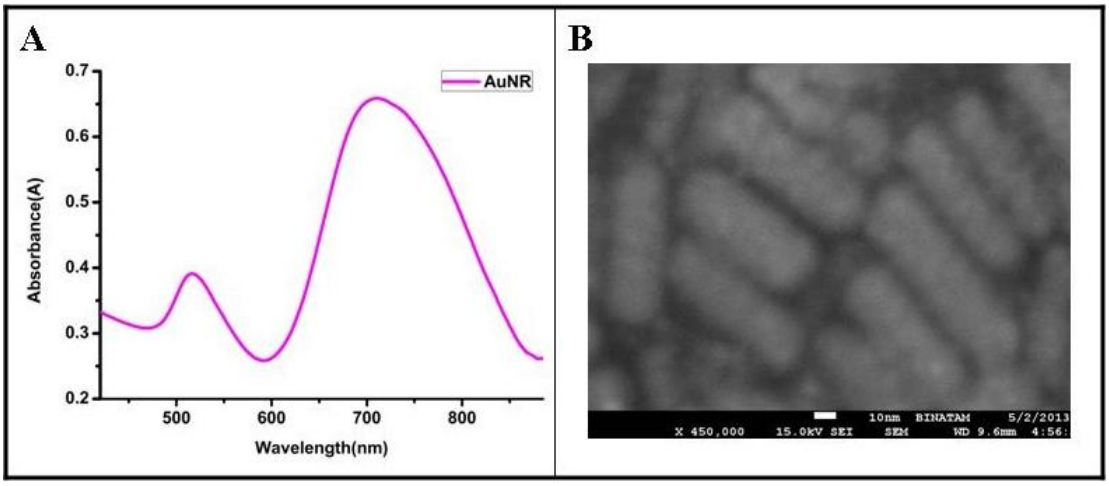

Figure 2.4 UV-vis spectra of AuNR with longitudinal absorption maxima at 710 nm, and transverse absorption maxima at 514 nm (a), SEM image of AuNR~60 nm (b).

2.1.3 Surface Modification of AuNPs

AuNS, AuNC, and AuNR were synthesized with 40 nm, 50 nm, and 60 nm sized respectively to use in imaging of MCF-7 (breast adenocarcinoma) and hMSC (human mesenchymal) cell lines by dark-field microscopy. To make the particles biocompatible, PEGylation was performed and to conjugate the antibody, DDA functionalization was done on the AuNPs with desired ratios (see Figure 2.5).

2.1.3.1 PEG and DDA Surface Functionalization

For 60% surface coverage of AuNPs with methyl-poly(ethylene glycol) thiol (mPEG-SH), and 40% coverage with 4,4'-dithiodibutyricacid (DDA); 0.0117 mM PEG-SH and DDA solutions were prepared. For desired percentages, 9 mL of each AuNPs were used and cleaned proper times and rates with DI water then re-suspended in 2 mL of DI water. For PEGylation, 3 mL of PEG solution was added and waited for 24 hours at room temperature with continuous stirring. For DDA conjugation, the PEGylated AuNPs were cleaned once at 13500 rpm for 15 min and re-suspended in 1 mL DI water, and then 3 mL DDA solution was added and waited overnight.

For the conjugation of DDA and activation of the carboxylic groups; AuNP-PEG-DDA solutions were centrifugated at 13000 rpm for 15 min and collected in 2 mL

DI water, then 2 mL, 1 mM of *sulfo*-NHS solution was added and waited for an hour. Then, the solution was cleaned at 13000 rpm for 15 min and re-suspended in 2 mL in DI water and then 2 mL EDC.HCl was added and waited for a hour with continuous stirring. Finally, all solutions were cleaned from excess materials by centrifugation at 13000 rpm for 15 min.

2.1.3.2 Antibody (HER-2) Conjugation

For the conjugations of AuNS-PEG-DDA, AuNC-PEG-DDA, AuNR-PEG-DDA, 5 mL of each AuNP was mixed with 20µL of anti-HER2 and left for 24 hrs for complete conjugation. Then, to remove excess antibody, centrifugation was applied at 6000 rpm for 15 min. Finally, it was re-suspended with 5 mL DMEM solution for cell study and UV-vis absorbance of each AuNP-PEG-AB combinations in DMEM were measured before cell incubation.

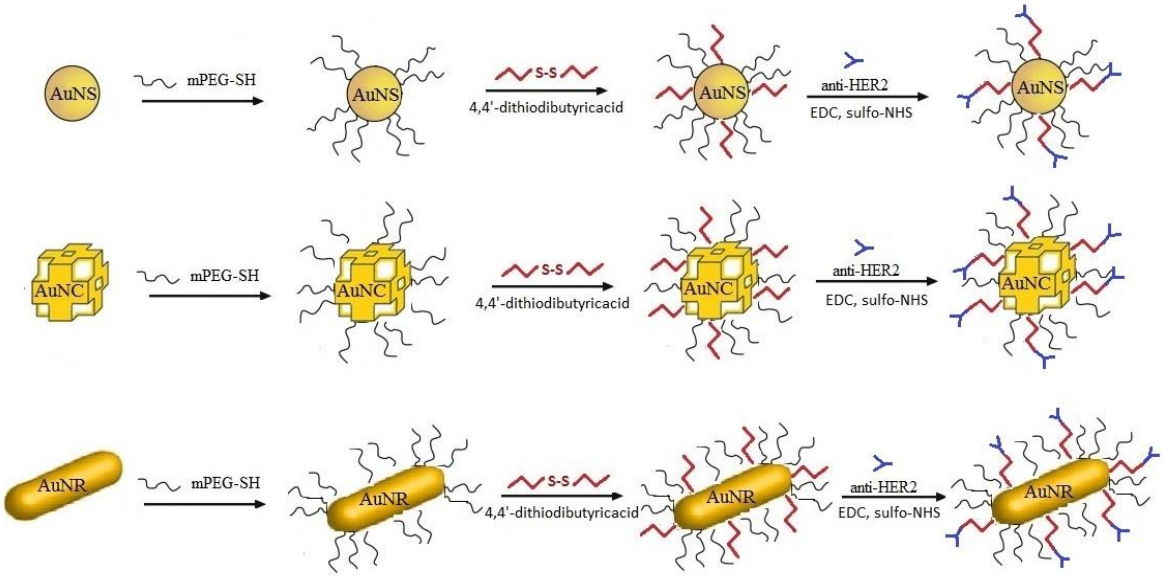

Figure 2.5 Schematic representation for preparation of nano-imaging system with gold nanoparticles which were conjugated with anti-HER2.

2.1.4 Bioimaging of MCF-7 and hMSC cells

2.1.4.1 Cell Study

MCF-7 cells were seeded a $1.4x10^5$ cells/well while hMSC lines were seeded $3.5x10^4$ cells/well in 1 mL culture medium. After 24 hrs, both cell lines were incubated with AuNPs. After 48 hrs incubation, the growth media which contains excess amount of AuNPs were collected to measure the absorbance differences before and after incubation to evaluate the cellular uptakes.

2.1.4.2 UV-vis Measurements

The cellular uptake and/or surface localization availability of the PEG-AuNPs and PEG-AB-AuNPs were monitored for both MCF-7 and hMSC cells. For analysis of cellular uptake efficacy of the AuNPs, the SPR spectra of the NPs were taken before and after the incubation with AuNP-PEG and AuNP-PEG-AB. The amounts of the AuNPs interacted with cells were evaluated according to the average number of cells on the slits and the absorbance differences of AuNPs before and after incubation. The total number of cell for each slits and absorbance differences were normalized to *absorbance difference/100 cells.*

2.1.4.3 Dark-Field Imaging

After UV-vis measurements, cells were fixed with 4% paraformaldehyde and used for dark-field imaging. For dark-field imaging, dark-field condenser was used in light microscope to make the light beam focused on the sample to scatter the light on the surface of the metal nanoparticles which were gold nanoparticles in our case.

2.2 THERAPEUTIC STUDY WITH AuNPs

AuNS was used as therapeutic agent to suppress the MMP-15 (matrix metalloproteinases 15) gene in HeLa (cervical carcinoma) cells with transfection of siRNA. For desired transfection covalently bonded PEI (poly ethylenimine) on the surface of the AuNS is thought to be safe and nontoxic platform to carry the gene and silence the MMP-15 is the enzyme known for its role in the invasion of tumour cells. In this study, we demonstrated suppressing of MMP-15 expression in HeLa cells by using

PEI conjugated gold nanosphere (AuNS) in safe way without any biodegradation and toxicity. The cell internalization of AuNS-PEI-siRNA complexes was monitored by dark-field imaging and gene silencing was followed by RT-PCR (reverse transcription polymerase chain reaction) analysis.

2.2.1 Materials

The hydrogen tetrachloroaurate ($HAuCl_4$), 4,4'-dithiodibutyricacid (DDA), sulfo-NHS, 2-mercaptoethanol, dimethylfloramine(DMF) were obtained from Sigma-Aldrich, Germany. EDC.HCl and sodium sulfide (Na_2S, 99%) were purchased from Alfa Aesar, Germany. Sodium citrate dihydrate ($C_6H_5Na_3O_7.2H_2O$) (SAFC, Austria), poly(ethyleneimine) (PEI) (Fluka) were purchased. All aqueous solutions were prepared with deionized (DI) water (18.2 MΩ.cm @ 25°C).

2.2.2 Surface Modification of AuNS

AuNS was synthesized with the same method which was described in section *2.1.2.1*. To make the nanoparticle compatible for gene delivery, necessary surface modifications were performed. Thiolated-PEI was used as cationic platform on the surface of the AuNS to make the carrying of the negatively charged siRNA possible.

2.2.2.1 Thiolation of PEI

0.059g of (0.025 mmol) of DDA was taken and dissolved in 12.5 mL of 0.0748g (0.065 mmol) sulfo-NHS dissolved and 1.5 mL dimethylfloramine included solution. After 2 hrs at room temperature with continuous stirring at 500 rpm, 0.1g of (0.055 mmol) of EDC.HCI which was dissolved in 10 mL DI water was added into previously prepared solution and waited for an hour. Then, prepared solution was added slowly into 0.25g of PEI dissolved 20 mL of solution with stirring and left overnight. After conjugation of PEI was provided with bis-(N-Hydroxysuccinimido)-4,4'-dithiodibutyrate, 224 μL of 2-mercaptoethanol was added and reacted for 2 hrs. Finally, prepared solution was purified overnight by dialysis (1000-Da cutoff).

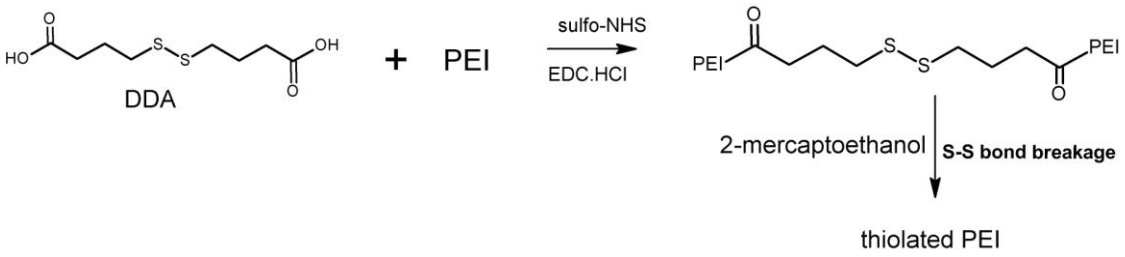

Figure 2.6 Schematic illustration for synthesis of thiolated PEI.

2.2.2.2 Conjugation of Thiolated PEI to AuNS Surface and siRNA Loading

Before AuNS was conjugated with thiolated PEI, had been cleaned from excess citrate by centrifugation at 8000 rpm for 15 min and resuspended with 10 mL DI water again. Then 100 μL of thiolated PEI was added to the AuNS solution and left overnight. AuNS-PEI colloid was centrifugated at 7500 rpm for 15 min and resuspended with 10 mL DI water.

siRNA Loading

After SPR of AuNS-PEI had been analyzed (see Figure 1a, 1c), 100 μL of 5 μM siRNA was added and mixed at 100 rpm for 24 hrs. For cell study and zeta analyze (see Figure 1d); to remove the excess siRNA, it was centrifugated at 7000 rpm for 15 min and resuspended in needed DMEM solution, growth medium, for gene silencing study in HeLa cells and UV absorbance was measured before cell incubation.

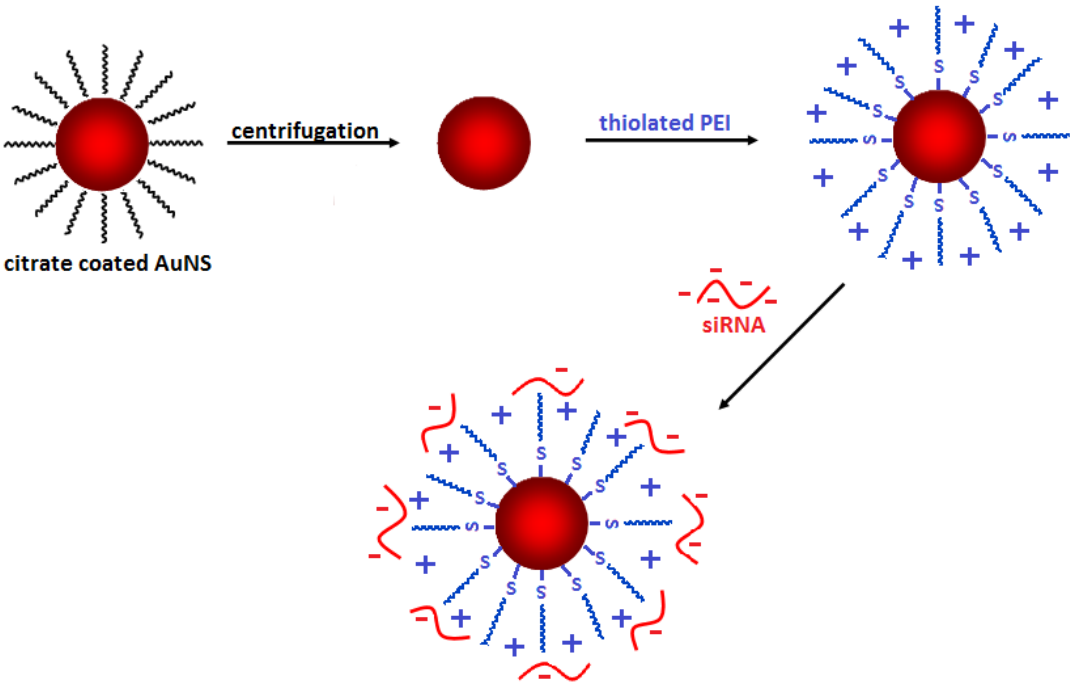

Figure 2.7 Representation of nanovehicle modification with PEI-SH and siRNA loading via electrostatic interaction.

2.2.3 Gene Silencing in HeLa Cells

2.2.3.1 Cell Study

Shortly, HeLa cells were seeded in a 6 well-plate at a density of $1x10^6$and were cultured overnight in a humidified incubator (5% CO_2, 37 ^oC). The next day, when the confluency of the cells reached 80-90%, transfection protocol was performed. First, specific siRNA (20µM each) were diluted to 2 µM with DNase/RNase free ddH2O. 200 µl, 2 µM siRNA and 200 µl DMEM (serum and antibiotic free) in one tube and 10 µl DharmaFECT and 390 µl DMEM in the other tube were prepared as transfection reactants for each transfection as a positive control, and the tubes were left at room temperature for 5 min. Then, the reactants were mixed and left at room temperature for 20 min. Finally, the transfection reactants were mixed with 1.5 ml DMEM (serum and antibiotic free) and applied to the cells which were left for incubation in a humidified incubator. For siRNA transfection study, 1 mL siRNA loaded AuNS-PEI solution was added to the cell media and left overnight in a humidified incubator (5% CO_2, 37 ^oC). 24 h after the transfection and gene expression analysis were performed.

2.2.3.2 RT-PCR Analysis

Degree of the mRNA transcripts encoding MMP-15 and GAPDH (housekeeping gene, internal control) genes were determined by RT-PCR. RNA was extracted from the cells according to the manufacturer's instructions (Roche High Pure RNA isolation Kit).cDNA was synthesized using an oligo(dT)18 primer according to the RevertAid™ First Strand cDNA Synthesis Kit's manual (Thermo Inc., MD). The amplification MMP-15 primers were used. After PCR reaction product were separated on a 1.5% agarose gel, stained with ethidium bromide.

2.2.3.3 Cytotoxicity Assay

Human HeLa cells were grown in Dulbecco's modified Eagle's medium (DMEM) with 10% fetal bovine serum (FBS). The cells were routinely maintained on plastic tissue culture dishes (Grainer) at 37°C in an incubator under a humidified atmosphere containing 5% CO2. All media routinely contained antibiotic–antimycotic agent (Biochrome). The cytotoxicity of the polymers was analyzed by 3-(4,5-dimethylthiazol)-2,5-diphenyltetrazolium bromide (MTT) assay. HeLa cells were seeded in a 96-well tissue culture plate at 10^6 cells per well in 90 μL DMEM medium containing 10% FBS. Cells achieved 70% confluence after 24 h. The medium was replaced with fresh DMEM medium. The AuNP were added to the cells with various concentrations (0.125 μM–1.25 μM) and incubated for 24 h at 37°C. Then, the mixture was collected for UV measurement and replaced with 100 μL of fresh DMEM medium supplemented with 10% FBS. After incubation, 10 μL of 2 mg/mL MTT solution in PBS was added. The cells were incubated for an additional 4 h at 37 °C, and then the medium was removed and 150 μL of dimethylsulfoxide was added to each well to dissolve the formazan crystals formed by living cells. Absorbance was measured at 570 nm using a microplate reader and recorded as a percentage relative to untreated control cells according to the following equation (2.1):

$$\text{Cell viability (\%)} = OD570^{(\text{sample})} / OD570^{(\text{control})} * 100 \qquad (2.1)$$

2.2.3.4 Dark-Field Imaging

HeLa cells which were incubated with siRNA loaded AuNS-PEI nanovehicles for 24 hrs at 37°C were fixed with 4% formaldehyde after growth media had been removed. After 20 min, cells were washed with DI water and dark-field images were taken by Leica microscope with dark-field condenser apparatus.

CHAPTER 3

RESULTS AND DISCUSSIONS

3.1 DIAGNOSTIC STUDY WITH AuNPs

3.1.1 Characterization and Surface Modifications of AuNPs

To identify the sizes and geometries of localized surface plasmon resonances of synthesized gold nanoparticles, UV-vis spectra and SEM images were investigated. According to the SEM images, the sizes of gold nanosphere (AuNS), gold nanocage (AuNC) and gold nanorod (AuNR) were estimated as, 40nm, 60 nm and 70 nm respectively (see Figure 2.1b, 2.2b, and 2.3b). The AuNPs must be biocompatible during the cellular interactions. To do this all the AuNPs were coated with mPEG-SH with the 60% surface coating (PEGylation).

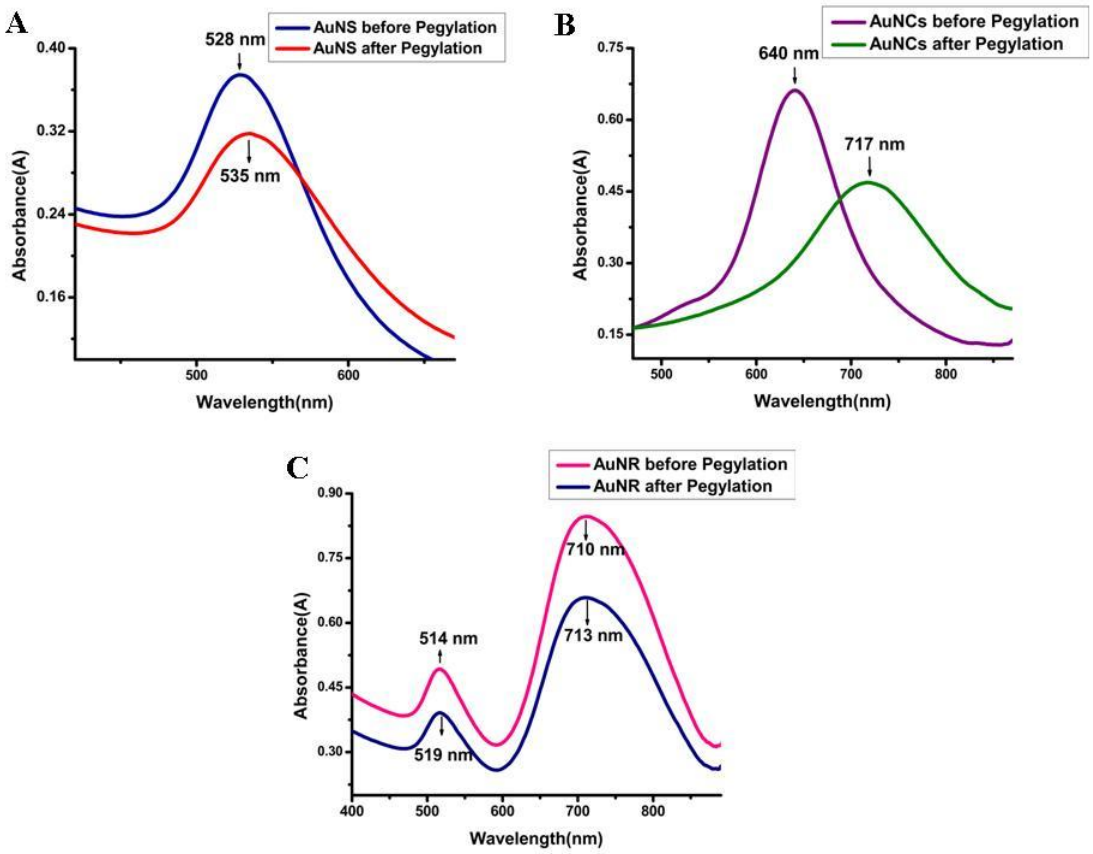

Figure 3.1 UV measurements of each of the AuNPs before and after PEGylation process.

PEGylation of surface results the bathochromic shifts in surface plasmon spectra of the nanoparticles (see Figure 3.1a, b, c). AuNS has 528 nm LSPR energy before PEGylation and 535 nm after the process. SPR shifting for AuNS is about ~7nm since the oscillation of the electrons in the conduction band through the spherical shape of the nanoparticle restricts the surface plasmon resonance. As a result, the LSPR is not so affected by the surface PEGylation on the spherical nanoparticle. However, the LSPR spectrum of the AuNC is highly bathochromic shifted by the surface PEGylation (from 640 nm to 717 nm which is about ~77 nm shifting). The reason for this, the corner of the cage is mostly responsible for the LSPR peak as the oscillation mostly occurs at corners. When the surface of the nanocage is PEGylated, the PEGylation mostly takes place on the corners of the nanocages, which results very large shifting of the SPR peak. On the other hand, the LSPR of the AuNR is not so affected by the PEGylation (710 nm to 713 nm about ~3nm shifting). This can be explained as the LSPR of the nanorod mostly occurs at

the tips as the oscillation mostly occurs at the tips of the rod. When the nanorod is PEGylated, very less amount of PEGylation takes place at the tips may be still the presence of the CTAB but largely along longitudinal. Because of this the LSPR spectrum of the AuNR is very less bathochromically shifted.

The anti-HER2 conjugations were achieved via the DDA linker on the AuNPs. The DDA were first attached on the AuNPs surface with the 40% surface coating and the anti-HER2 antibody (AB) was coupled in the presence of EDC and *sulfo*-NHS. To obtain the more antibody conjugation we coated the surface of the nanoparticles with more amount of the DDA linker (about 40%). We believe that, the more amount of antibody on the NP surface may also enhance the solubility and as well as the biocompatibility (see Figure 2.5). The fixation of the antibody on the surface of the AuNPs prevents unwanted unloading of antibody during the cellular interaction and enhances the uptake ability of the nanoparticles. Because the free unloaded antibodies in the medium may block the cell surface receptors and this may not allow the NP interactions with cells.

3.1.2 The Cellular Interactions of AuNPs and Dark-Field Imaging

The cellular uptake and/or surface localization availability of the PEG-AuNPs and PEG-AB-AuNPs were monitored for both MCF-7 and hMSC cells. For analysis of cellular uptake efficacy of the AuNPs, the LSPR spectra of the NPs were taken before and after the incubation with AuNP-PEG and AuNP-PEG-AB. The amounts of the AuNP interacted with cells were evaluated according to the average number of cells on the slits and the absorbance differences of AuNPs before and after incubation (see Figures 3.2 and 3.3). The total number of cell for each slits and absorbance differences were normalized to *absorbance difference/100 cells.*

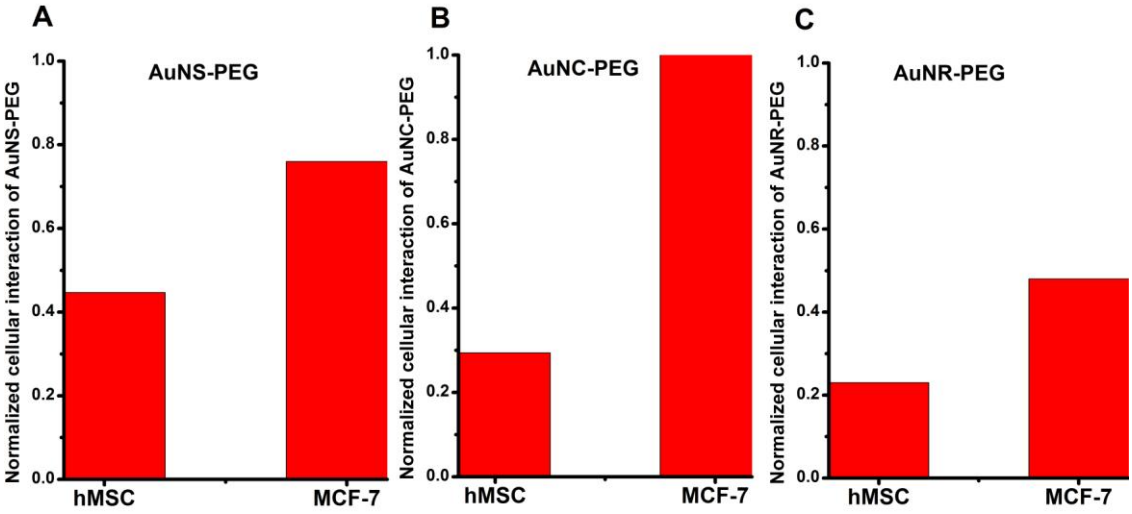

Figure 3.2 Normalized cellular interactions of AuNS-PEG (a), AuNC-PEG (b), AuNR-PEG (c), with hMSC and MCF-7 cell lines.

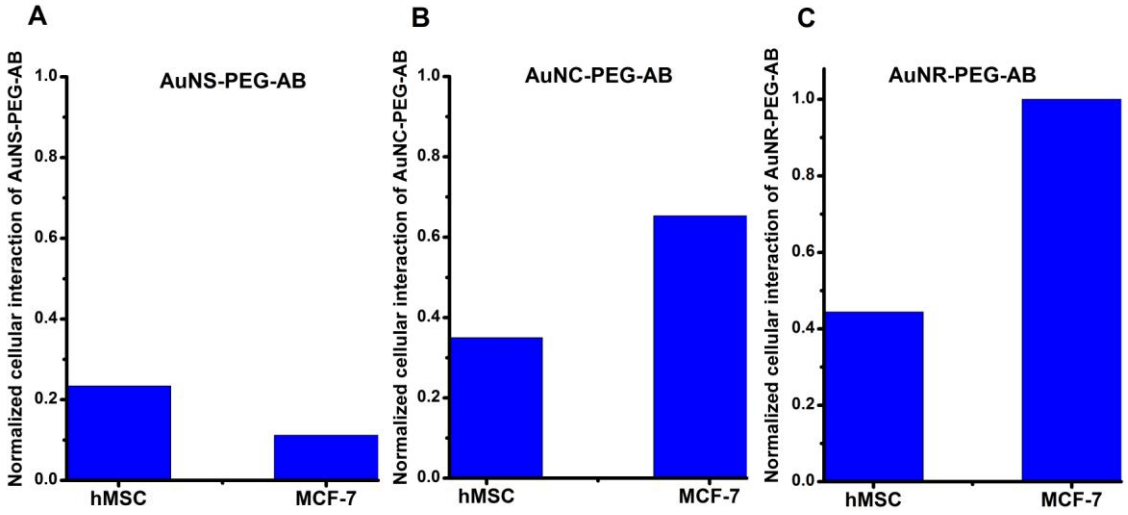

Figure 3.3 Normalized cellular interactions of AuNS-PEG-AB (a), AuNC-PEG-AB (b), AuNR-PEG-AB (c); with hMSC and MCF-7 cell lines.

The cell internalization and cellular accumulation of the nanoparticle platforms can occur based on an active or a passive mechanism. In the active mechanism, the targeting molecules such as antibodies, peptides, or small molecules are used to recognize the specific cell surface receptors on the tumour cell. In this method, the nanoparticle internalization can be performed by receptor-mediated endocytosis. In the passive mode, the nanoparticles without targeting molecules are accumulated and

retained in the tumor interstitial space mainly through the enhanced permeability and retention effect. [55]

The active endocytosis of NPs depends on shape, size and surface coatings with antibody (anti-HER2 antibody is mostly found in breast cancer (MCF-7)). In both mechanisms, cancer cells have extremely high potential for endocytosis of biomolecules or biocompatible nanoparticles. In this part, we have compared the cellular interactions of anti-HER2 targeted AuNPs with non-targeted AuNPs. All AuNPs were PEGylated to make them biocompatible. When the cellular interactions of non-targeted AuNPs-PEG with MCF-7 (cancer cells) and hMSC (noncancerous cells) are compared, we have found that all shaped AuNP-PEGs (AuNS, AuNC and AuNR) have higher interaction with cancer cells than normal cells (see Figure 3.2). This can be attributed to the strong endocytosis efficiency of the cancer cells to promote the cell viability and cell proliferation. However, among these, AuNR has the lowest cellular interaction than the others because of the bigger size and the longer shape compared to others which may reduce the enhanced permeability and retention effect.

When we compare receptor-mediated endocytosis or cellular interaction of the antibody targeted AuNPs (AuNPs-PEG-AB) with MCF-7 and hMSC cells, we found that AuNS-PEG-AB has lowest cellular interaction with MCF-7 when it is compared to others. (see Figure 3.3). The reason for this might be the small size and spherical shape of AuNS may reduce the cross-section of the particle shape attached on the cell surface which results the less amount of antibody interacted with the cell receptors. This also supports that why the non-targeted AuNS has much more cellular interaction with MCF-7 than antibody targeted AuNS. This result implies that AuNS can provide efficient cellular internalization than other shaped NPs. When the shapes are compared we found that antibody targeted AuNR has the highest cellular interaction with surface receptors of MCF-7 cells (see Figure 3.4).

This can be explained by the bigger size and longer shape results more cross-sections on the cell surface and more antibody conjugation on the nanoparticle give more interaction with receptors which results greater membrane wrapping time required for the elongated particles (see Figure 3.4).

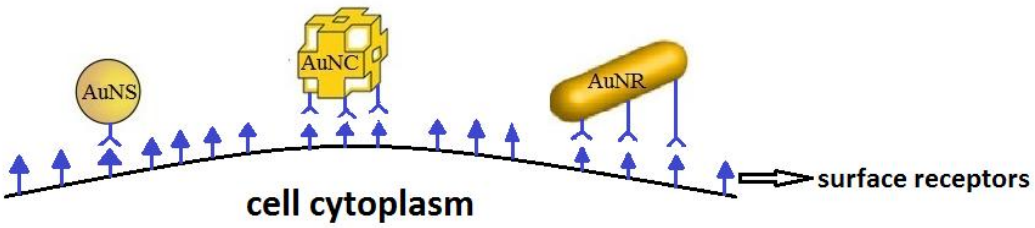

Figure 3.4 Cross sections of three different shaped AuNP-PEG-AB.

The cellular interaction of AB targeted and non-targeted AuNPs with MCF-7 and hMSC were monitored by dark-field imaging microscopy without using any dye to investigate the efficiencies of different shaped AuNPs in imaging and cellular internalization. We used the optical microscope which was equipped with a dark field condenser to collect the scattered light only from the sample. The cellular uptake and/or surface localization availability of the PEG-AuNPs and PEG-AB-AuNPs were monitored for both MCF-7 and hMSC cells (see Figure 3.5). The dark- field images clearly reveals that the PEGylated nanoparticles have better interactions with cancerous cells than noncancerous cells. However, when the nanoparticles are conjugated with antibodies the cellular interaction of targeted nanoparticles with cancerous cells increase. From the figures, it is obvious that AuNC and AuNR have more bright appearance than AuNS because of high light scattering of the nanoparticles on the corners and the tips (see Figures 3.5f,g,i,k) and the cellular uptake of AuNS is more clear than other nanoparticles due to its spherical shape which makes them easy to endosomal uptake (see Figure 3.5a).

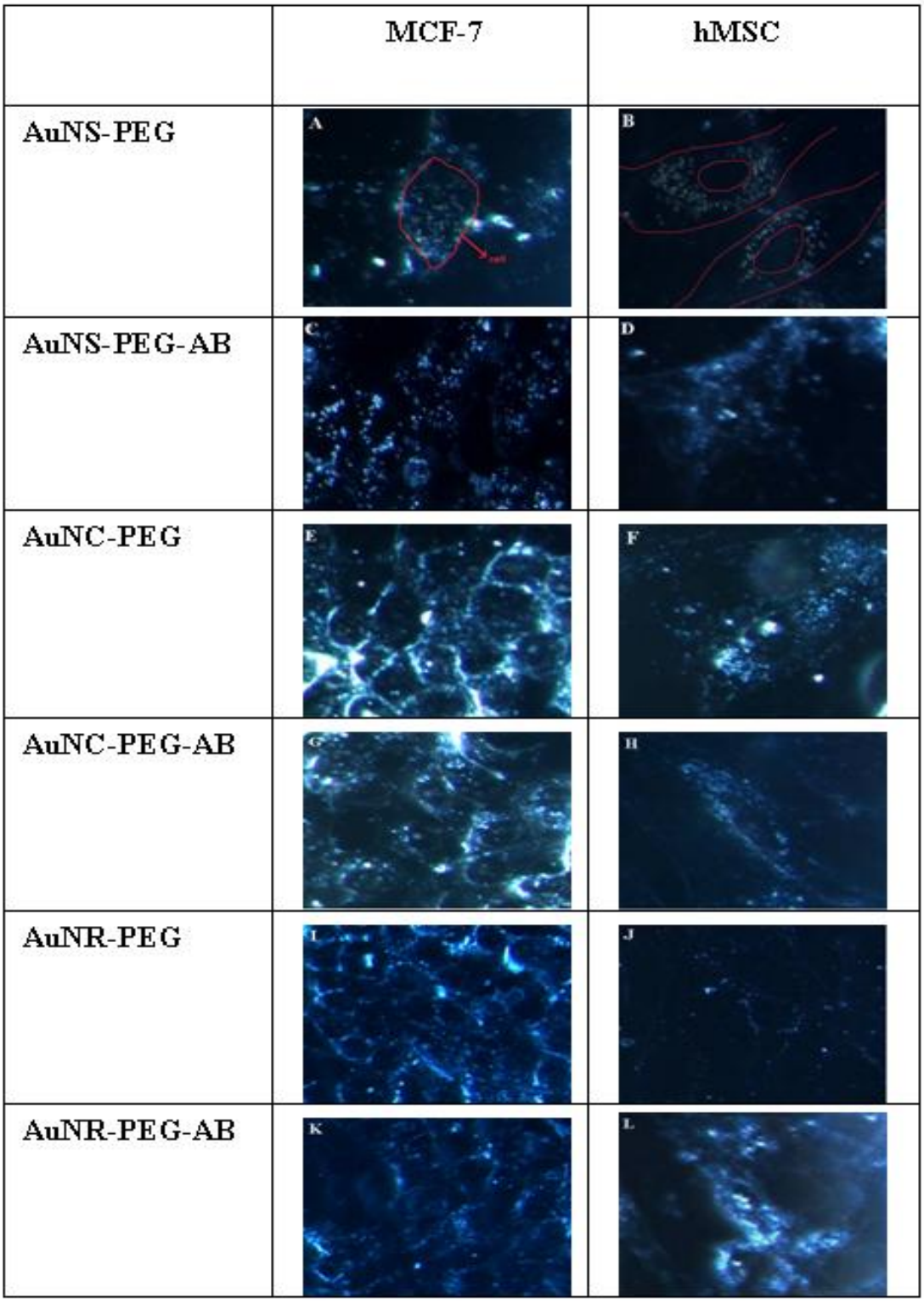

Figure 3.5 Dark field images of cancer cells (MCF-7) and normal cells (stem cell, hMSC) which were treated with anti-HER2 conjugated and PEGylated different types of AuNPs.

3.2 THERAPEUTIC STUDY WITH AuNPs

In this part of the study, we aimed to design stable, efficient and biocompatible nanovehicle for both therapeutic and diagnostic applications by carrying the MMP-15 siRNA in the HeLa cells monitoring with dark-field microscopy. MMP-15 is one of the genes which are responsible from invasion of the tumor cells. The significant point here is to design a suitable carrier for MMP-15 siRNA transfection.

In that regard, AuNS which is a plasmonic metal nanoparticle was used as nanovehicle's center part, providing the monitoring of the transfected siRNA by dark-field microscopy. PEI was chosen as cationic and biocompatible polymer to cover the surface of AuNS to carry the negatively charged siRNA in cancer cells by electrostatic interaction. In addition, covalent conjugation between thiolated-PEI and AuNS was executed via sulphur-gold covalent interaction (bonding) to prevent undesirable releasing of polymer in cell environment and to enhance the efficacy of transfection by increasing the capacity of loaded siRNA. Another reason of using PEI layer on AuNS is to make the escape of loaded siRNA possible when it enters the cell. This should happen due to the acidity difference between cancer cell and outer media.

3.2.1 Characterization and Surface Modification of AuNS

AuNS was chosen as the nanovehicle for siRNA delivery because of its high internalization ability which was observed in previous part (*in diagnostic study*) and it was synthesized with same procedure in that part using the Turkevich method. The size of the AuNS can be tuned by changing the synthesis parameters like concentration of gold solution or citrate, stirring rate and temperature. The synthesized AuNS in this study has 523 nm absorption maxima which indicates 27 nm size (see Figure 3.7a). The size of the particle was also analyzed by using Transmission Electron Microscopy (TEM) images which indicate approximately 20 nm sized particles and zeta measurements which point out 27 nm sized particle distribution in colloid system (see Figure 3.7b, c, d). Consequently, it is defensible to say that the size of used AuNS is around 25 nm.

PEI was used as positively charged layer on AuNS to carry negatively charged genes into the cancer cells. Thiolation of PEI was performed (see Figure 2.6) to attach the positive layer to the gold surface. After PEI had been coated on the surface of the

AuNS, UV-vis measurement of AuNS-PEI was analyzed (see Figure 3.6a). When the surface energy of plasmonic nanoparticles changes by conjugation or interaction with any molecule, they have shifts in their LSPR bands. In AuNS-PEI conjugation, betachromatic LSPR shifting in UV measurement was observed from 523 nm to 531 nm which indicated the success of proper conjugation of PEI to AuNS surface via covalent bonding (see Figure 3.6a).

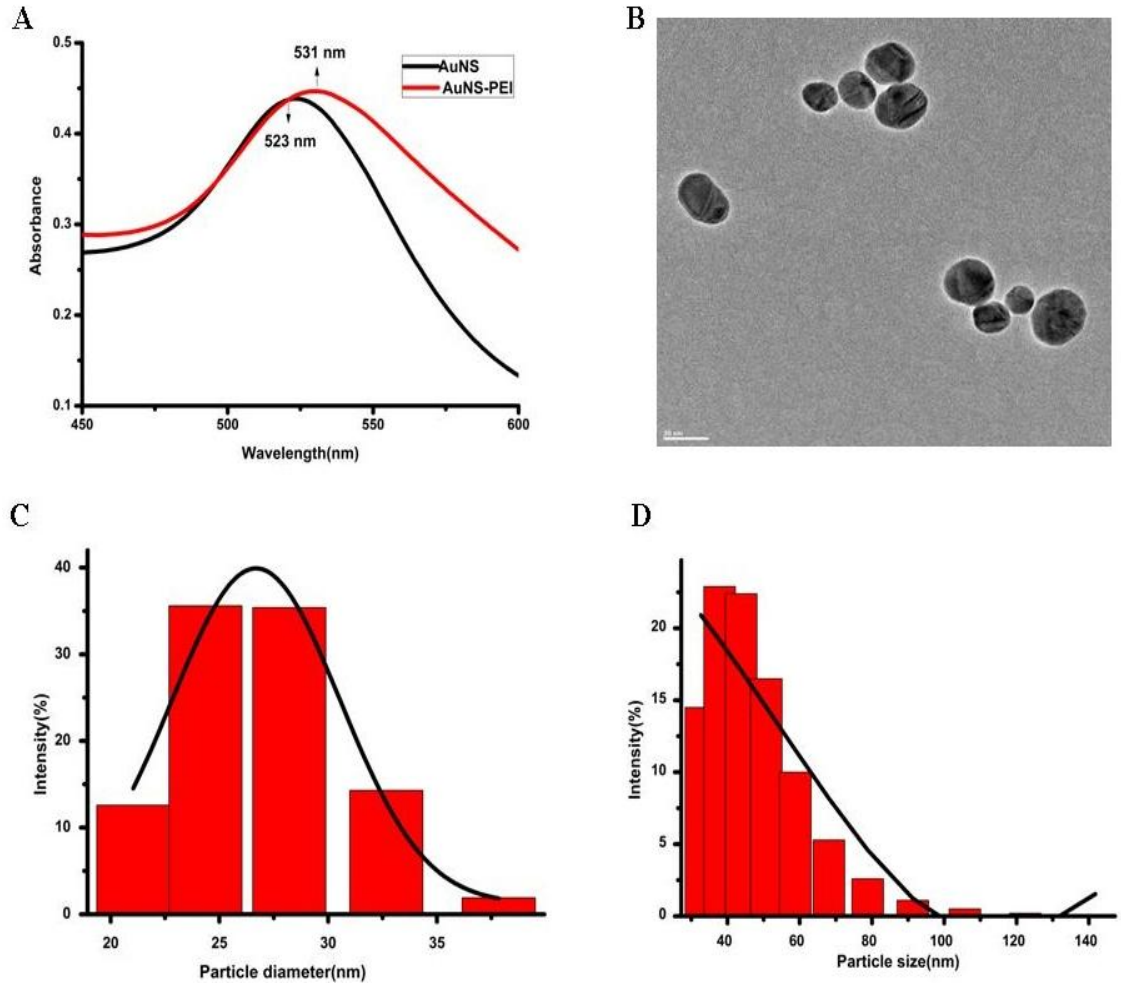

Figure 3.6 LSPR spectra of AuNS and AuNS-PEI (a), TEM image of AuNS~20 nm (b), and zeta potentials of AuNS-PEI (c) and AuNS-PEI-siRNA (d).

The surface modification of AuNS was also analyzed by getting zeta potential. The size of PEI coated AuNS has bigger size around 45-50 nm (see Figure 3.7d). Beside the cationic property of PEI, its polymeric structure has advantages to make the nanoparticle suitable sized to collect the scattered light in dark-field imaging system and

to provide ease transfection into HeLa cells. Because, it is known that the size of the nanoparticle should be larger than 30 nm for successful dark-field images by collecting the scattered light. The size and surface charge of AuNS-PEI and AuNS-PEI-siRNA conjugations were analyzed by using zeta potential analyzer (see Figure 3.6c, d). It was seen that particle sizes got higher when PEI was conjugated and siRNA was loaded.

3.2.2 siRNA Delivery, Uptake and Release Mechanisms

Delivery of the siRNA can be provided by using several methods and vehicles. Mostly used methods have some limitations in capacity of carrying and releasing of the siRNA inside of the cell. To overcome these limitations, some smart vehicles are worked on to design by many scientists to enhance the therapeutic applications of siRNAs. In nanotechnology, several types of nanoparticles are used as carriers of genes, drugs, biomarkers, and biomolecules to the target cell or tissue. In siRNA technology, successful transportation of genes into the cell is the heart of the studies. Because siRNAs can not enter the cells by themselves, they need a stable, biocompatible, easy synthesized and cheap vehicle to get inside of the cell to interrupt the working of desirable genes. Liposome based nanoparticles, magnetic nanoparticles, gold nanoparticles and quantum dots are some examples of nanovehicles used in systemic delivery of siRNA in therapeutic studies.

siRNA is collaborated with nanoparticles either through chemical linkage via covalent bonds or through non-covalent interactions like electrostatic interaction which performed in our study. Nanoparticles facilitate cellular uptake of siRNA cargo the process that commonly occurs through three main pathways (a) membrane fusion, (b) receptor-mediated endocytosis, and (c) direct endocytosis (see Figure 3.8). The mechanism of internalized siRNA is controlled and initiated by the interaction with RNA-induced silencing complex (RISC). The remaining antisense strand recognizes the homologue region with base-pairing and degrading the target mRNA resulting in inhibition of gene expression.

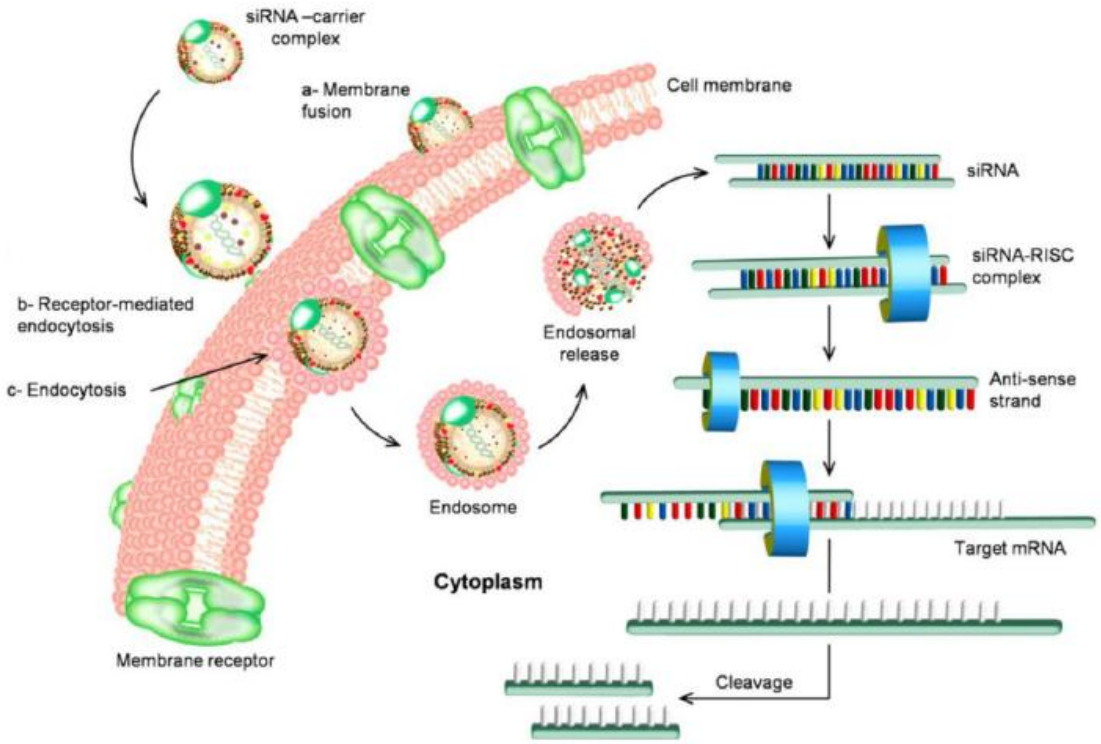

Figure 3.7 Gene silencing mechanism by using siRNA. [56]

In our study, AuNP was used as nanovehicle which was covered with PEI polycationic polyamine. PEI itself is widely used as nucleic acid delivery vehicle because of its ability to accept the protons pumped into endolysosomes. PEI could increase the pH of the endosome by accepting the protons. When pH is increased in endosome, degradative enzymes are inactivated in endolysosomes to alter protein folding. By using this pH responsive property of PEI, endolysosomal escape of delivered biomolecule (DNA, siRNA, etc.) becomes possible and cargo eventually reaches the cytoplasm or nucleus for many purposes. In addition, PEI/siRNA interaction is important to prevent any protein binding to the structure. Electrostatic interaction between positively charged PEI and negatively charged siRNA let them to neutralize each and by this way ease transfection without any protein aggregation or binding which could be due to the presence of any charge on the nanovehicle. On the other hand, free PEI harms the cells because of its permeable property on cell membrane. [57]

Many advantages are provided by using metal and cationic polymer based delivery system; i) by using AuNP based delivery system, non-degradable and stable vehicle has been designed, ii) the Au core which scattered the light during the dark-field imaging, monitoring of the vehicle in and out of the cell came possible and transfected siRNA loaded gold nanovehicle was monitored by this method, iii) branched-PEI was selected as cationic platform for siRNA delivery because of its cheep price, good stability in cell media to had efficient delivery, iv) PEI was attached to the surface of the AuNS covalently to prevent any unwanted PEI release which could cause toxicity in the cell, v) MMP-15 siRNA was loaded to AuNS-PEI platform electrostatically and release of the siRNA was possible when the pH of the media changed inside of the cancerous cell which let the PEI became more negative and broke the interaction of siRNA with PEI (endolysosomal escape) (see Figure 3.8).

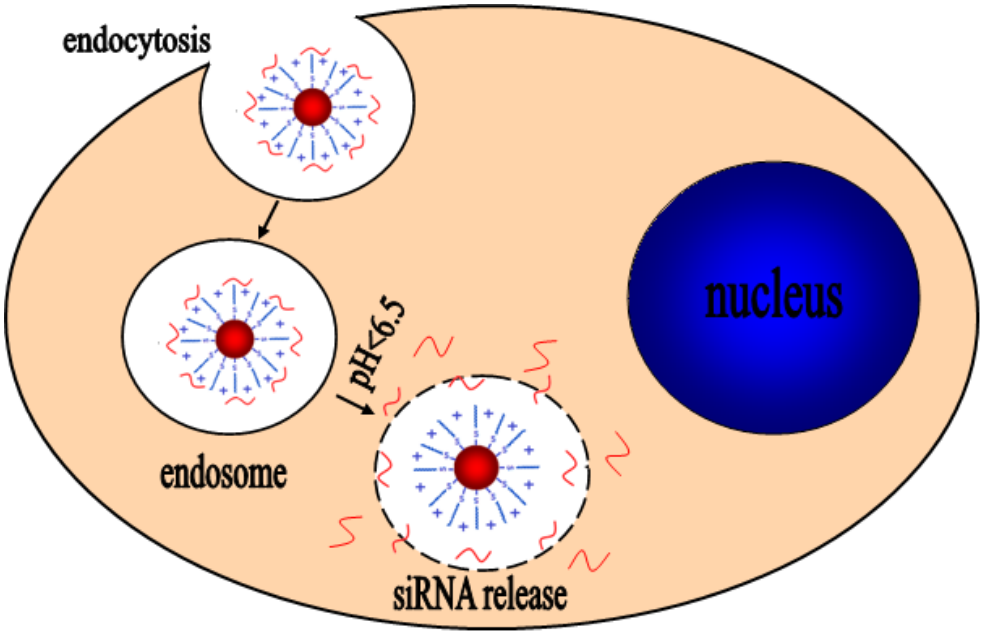

Figure 3.8 Uptake and release mechanism of siRNA loaded to AuNS in HeLa cell.

By conjugation of PEI to the AuNS covalently, weakly toxic effect of the PEI tried to be eliminated. Cytotoxic test was performed to assign the toxicity of the AuNS-PEI and AuNS-PEI-siRNA system, the cell viability was analyzed in different

concentrations (see Figure 3.9). It was seen that siRNA delivery to the HeLa cells to suppress the MMP-15 gene to prevent cancer invasion by using AuNS-PEI nanovehicle was mostly nontoxic until 0.5μM concentration which was very high than used concentration in the experiment.

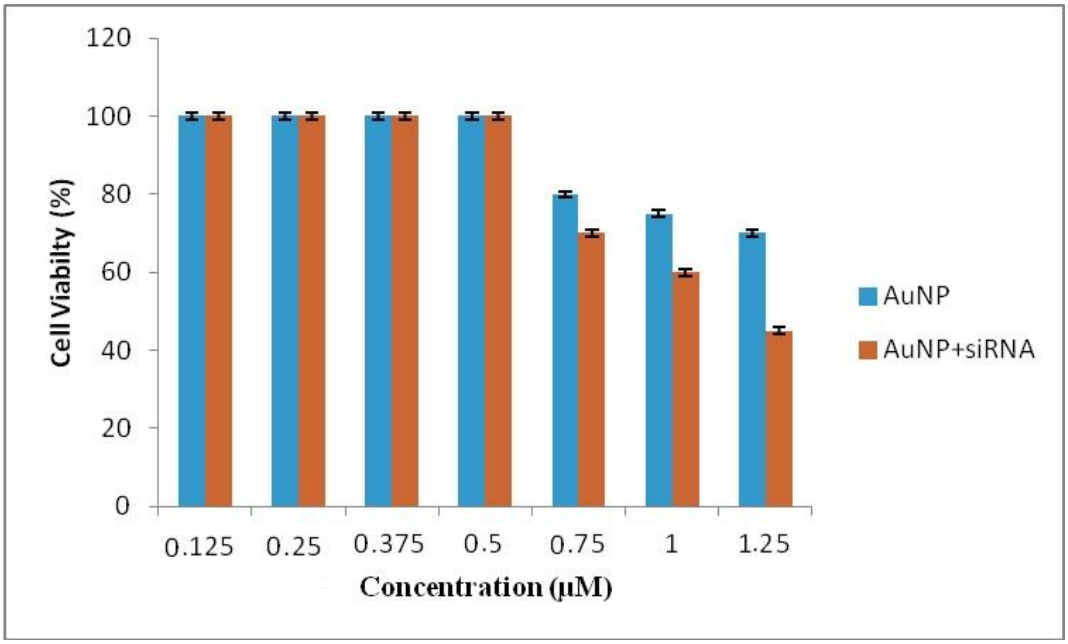

Figure 3.9 Cytotoxicity assay for AuNS-PEI-siRNA conjugation in HeLa cells.

3.2.3 MMP-15 Gene Knockdown and Dark-field Monitoring

Matrix metalloproteinases (MMPs) are the enzymes which take roles in the digestion of the extracellular matrix (ECM) components and in the stimulation of tumor growth, invasion, and metastasis [58]. MMP-15 is one of the members of this enzyme family and suppressing of this gene is vital for many disease treatments. Therefore, MMP-15 was chosen as target gene to knockdown by carrying its siRNA in HeLa cells with AuNS-PEI nanovehicle in our study. MMP-15 gene knockdown efficiency was analyzed by using RT-PCR technology. DharmaFECT which is a commercially available lipid-based transfection reagent was used as control in RT-PCR.

After transfections of siRNA with both DharmaFECT and prepared AuNS-PEI nanocarrier, 24 hrs incubation periods were applied and RT-PCR results pointed out that MMP-15 gene silencing was succesfully happened after 24 hrs by tranformation of the siRNA (see Figure 3.10).

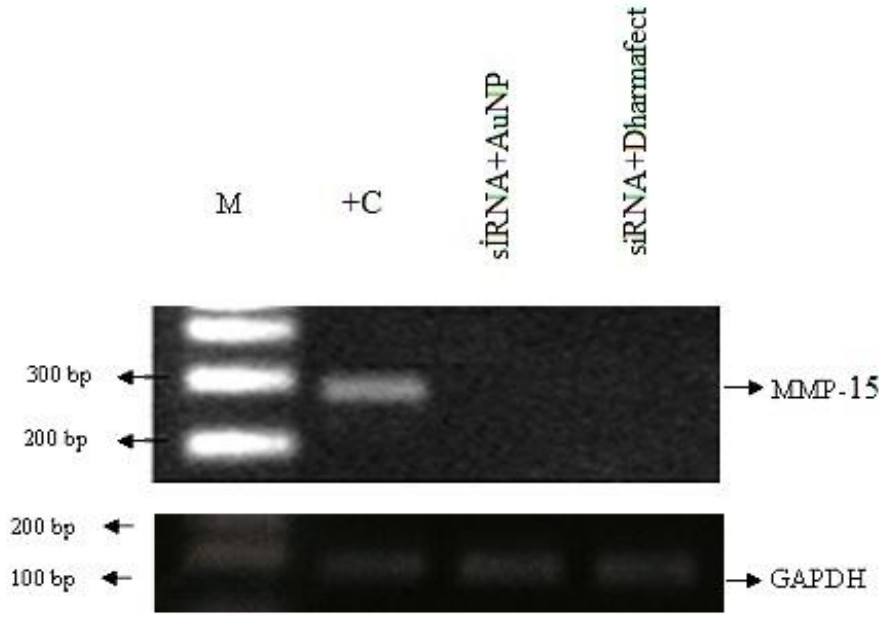

Figure 3.10 RT-PCR results as 2nd lane; HeLa cell and no transfection, 3th lane; HeLa cell+MMP-15 siRNA+ AuNP, 4th lane is HeLa cell+ MMP-15 siRNA+ DharmaFECT transfection reagent.

As a result, MMP-15 gene was knockdowned at gene level in HeLa cells when its siRNA was carried with AuNS-PEI nanotherapeutic reagent as sufficient as commercially used reagent, DharmaFECT.

In addition to the working principle as a siRNA cargo, AuNS-PEI can also work as a imaging reagent due to AuNSs LSPR which let it to scatter under dark-field microscopy. Dark-field imaging has advantages with its imaging capability in longer time period, imaging can be repeated because of fixation, rather than fluorescence probe used methodologies. In this study, dark-field imaging afforded to have images of AuNS-PEI-siRNA nanostructure after it hade been incubated with HeLa cells.

In conclusion, presence of AuNS in the cytoplasm of the HeLa cells were observed in dark-field images (red arrows in Figure 3.11 points the AuNS). Thus, imaging of HeLa cells guarantied that nanovehicles entered the cell successfully (see Figure 3.11).

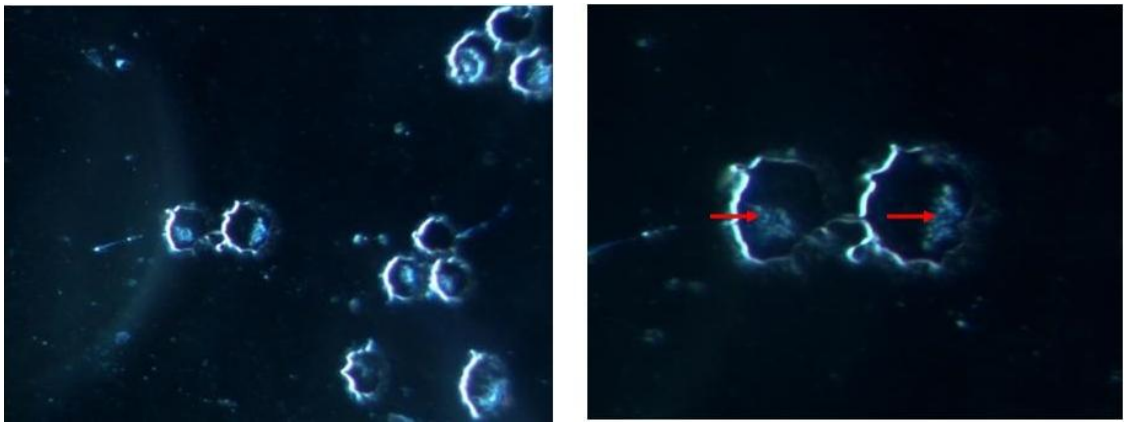

Figure 3.11 Dark-field images of AuNS-PEI-siRNA entered HeLa cells.

CHAPTER 4

CONCLUSION

In diagnostic work, three different shapes of AuNPs were synthesized and antibody (anti-HER2) modified AuNPs were studied for bioimaging and cellular uptake purposes. According to the SEM images, the sizes of AuNS, AuNC, and AuNR were estimated as, 40 nm, 60 nm, and 70 nm respectively. UV-vis and dark-field imaging were performed to investigate the efficiencies of different AuNPs. Cellular interactions of anti-HER2 targeted AuNPs with non-targeted AuNPs were performed by using absorbance differences between before and after incubation. From the dark-field images and normalized cellular interaction of AuNP-PEG and AuNP-PEG-AB conjugations with MCF-7 and hMSC, we concluded that AuNS is the better shaped nanoparticle for cellular internalization and biomolecule delivery purposes due to its spherical geometry, on the other hand AuNR and AuNC are better shaped nanoparticles for imaging due to their high cross-sections with the cell surface and high light scattering efficiencies.

In therapeutic study, AuNS-PEI-siRNA was designed as promising delivery system for transfection of siRNA to suppress the MMP-15 gene in HeLa cells. By analyzing the RT-PCR and cytotoxicity assay results, we can demonstrate that AuNS with cationic layer for negatively charged siRNA loading worked well to knockdown the gene by its abilities; (a) to pass through the cell membrane, (b) to load the siRNA and to transport it through the membrane and cytoplasm, (c) to discharge the gene in cytosol with pH response, (d) to exhibit no cytotoxicity and not to influence life processes taking place in the cells, (e) to monitor the entered AuNP-PEI-siRNA vehicle by dark-field microscopy.

REFERENCES

[1] Jemal, A., et al., *Cancer statistics, 2009.* CA Cancer J Clin, 2009. **59**(4): p. 225-49.

[2] Melixetian, M.B., et al., *Altered expression of DNA-topoisomerase II alpha is associated with increased rate of spontaneous polyploidization in etoposide resistant K562 cells.* Leukemia Research, 2000. **24**(10): p. 831-837.

[3] Brigger, I., C. Dubernet, and P. Couvreur, *Nanoparticles in cancer therapy and diagnosis.* Adv Drug Deliv Rev, 2002. **54**(5): p. 631-51.

[4] Kereselidze, Z., et al., *Gold nanostar synthesis with a silver seed mediated growth method.* J Vis Exp, 2012(59).

[5] B. Liu, J.X., J. Y. Lee, Y. P Ting, and J. Paul Chen, *Optimization of High-Yield Biological Synthesis of Single-Crystalline Gold Nanoplates.* J. Phys. Chem., 2005. **109**: p. 15256-15263.

[6] Ghosh, P., et al., *Gold nanoparticles in delivery applications.* Adv Drug Deliv Rev, 2008. **60**(11): p. 1307-15.

[7] Ozbay, E., *Plasmonics: merging photonics and electronics at nanoscale dimensions.* Science, 2006. **311**(5758): p. 189-93.

[8] Clemens Burda, X.C., Radha Narayanan, and Mostafa A. El-Sayed, *Chemistry and Properties of Nanocrystals of Different Shapes.* Chem. Rev. , 2005. **105**: p. 1025-1102.

[9] Chen, C.D., et al., *Sensing capability of the localized surface plasmon resonance of gold nanorods.* Biosens Bioelectron, 2007. **22**(6): p. 926-32.

[10] Rivera, V.A.G., F.A. Ferri, and E. Marega, *Localized Surface Plasmon Resonances: Noble Metal Nanoparticle Interaction with Rare-Earth Ions.* 2012.

[11] Pingarrón, J.M., P. Yáñez-Sedeño, and A. González-Cortés, *Gold nanoparticle-based electrochemical biosensors.* Electrochimica Acta, 2008. **53**(19): p. 5848-5866.

[12] Wu, Z., et al., *Activity-based DNA-gold nanoparticle probe as colorimetric biosensor for DNA methyltransferase/glycosylase assay.* Anal Chem, 2013. **85**(9): p. 4376-83.

[13] Mahmoud, M.A. and M.A. El-Sayed, *Metallic double shell hollow nanocages: the challenges of their synthetic techniques.* Langmuir, 2012. **28**(9): p. 4051-9.

[14] Li, J.H.Z.W.J., *Gold Nanoparticles With Special Shapes: Controlled Synthesis, Surface-enhanced Raman Scattering, and The Application in Biodetection.* Sensors, 2007. **7**(12): p. 32993311.

[15] Sperling, R.A. and W.J. Parak, *Surface modification, functionalization and bioconjugation of colloidal inorganic nanoparticles.* Philos Trans A Math Phys Eng Sci, 2010. **368**(1915): p. 1333-83.

[16] Astruc, M.-C.D.a.D., *Gold Nanoparticles: Assembly, Supramolecular Chemistry, Quantum-Size-Related Properties, and Applications toward Biology, Catalysis, and Nanotechnology.* Chem. Rev. , 2004. **104**: p. 293-346.

[17] Biju, V., *Chemical modifications and bioconjugate reactions of nanomaterials for sensing, imaging, drug delivery and therapy.* Chem Soc Rev, 2014. **43**(3): p. 744-64.

[18] David A. Giljohann, D.S.S., Weston L. Daniel, Matthew D. Massich, Pinal C. Patel, and Chad A. Mirkin, *Gold nanoparticles for biology and medicine.* Angewandte Chemie (International ed. in English), 2010. **49**(19): p. 3280-3294.

[19] DeSimone, R.A.P.a.J.M., *Strategies in the design of nanoparticles for therapeutic applications.* Nature reviews. Drug discovery, 2010. **9**(8): p. 615-627.

[20] Shi, J., et al., *Nanotechnology in drug delivery and tissue engineering: from discovery to applications.* Nano Lett, 2010. **10**(9): p. 3223-30.

[21] Pooja M. Tiwari, K.V., Vida A. Dennis and Shree R. Singh, *Functionalized Gold Nanoparticles and Their Biomedical Applications.* Nanomaterials, 2011. **1**(1): p. 3163.

[22] Lipka, J., et al., *Biodistribution of PEG-modified gold nanoparticles following intratracheal instillation and intravenous injection.* Biomaterials, 2010. **31**(25): p. 6574-81.

[23] Cho, W.S., et al., *Size-dependent tissue kinetics of PEG-coated gold nanoparticles.* Toxicol Appl Pharmacol, 2010. **245**(1): p. 116-23.

[24] Lee, S.H., et al., *Amine-functionalized gold nanoparticles as non-cytotoxic and efficient intracellular siRNA delivery carriers.* Int J Pharm, 2008. **364**(1): p. 94-101.

[25] Wangoo, N., et al., *Synthesis and capping of water-dispersed gold nanoparticles by an amino acid: bioconjugation and binding studies.* J Colloid Interface Sci, 2008. **323**(2): p. 247-54.

[26] Alexander G. Tkachenko, H.X., Yanli Liu, Donna Coleman, Joseph Ryan, Wilhelm R. Glomm, Mathew K. Shipton, Stefan Franzen,* and Daniel L. Feldheim, *Cellular Trajectories of Peptide-Modified Gold Particle Complexes: Comparison of Nuclear Localization Signals and Peptide Transduction Domains*, in *Bioconjugate Chemistry*2004. p. 482490.

[27] Rayavarapu, R.G., et al., *Synthesis and bioconjugation of gold nanoparticles as potential molecular probes for light-based imaging techniques.* Int J Biomed Imaging, 2007. **2007**: p. 29817.

[28] Surujpaul, P.P., et al., *Gold nanoparticles conjugated to [Tyr3]octreotide peptide.* Biophys Chem, 2008. **138**(3): p. 83-90.

[29] Kim, J.H., et al., *A functionalized gold nanoparticles-assisted universal carrier for antisense DNA.* Chem Commun (Camb), 2010. **46**(23): p. 4151-3.

[30] Rink, J.S., et al., *Transfection of pancreatic islets using polyvalent DNA-functionalized gold nanoparticles.* Surgery, 2010. **148**(2): p. 335-45.

[31] Javier, D.J., et al., *Oligonucleotide-gold nanoparticle networks for detection of Cryptosporidium parvum heat shock protein 70 mRNA.* J Clin Microbiol, 2009. **47**(12): p. 4060-6.

[32] Liu, Y., et al., *Single chain fragment variable recombinant antibody functionalized gold nanoparticles for a highly sensitive colorimetric immunoassay.* Biosens Bioelectron, 2009. **24**(9): p. 2853-7.

[33] Silva, J., A.R. Fernandes, and P.V. Baptista, *Application of Nanotechnology in Drug Delivery.* 2014.

[34] James Chen Yong Kah, K.W.K., Caroline Guat Leng Lee, Colin James Richard, Sheppard, Ze Xiang Shen, Khee Chee Soo, Malini Carolene Olivo, *Early diagnosis of oral cancer based on the surface plasmon resonance of gold nanoparticles.* International Journal of Nanomedicine, 2007: p. 785–798.

[35] Ivan H. El-Sayed, X.H., and Mostafa A. El-Sayed, *Surface Plasmon Resonance Scattering and Absorption of anti-EGFR Antibody Conjugated Gold Nanoparticles in Cancer Diagnostics: Applications in Oral Cancer.* Nano Lett, 2005. **5**: p. 829-834.

[36] Linlin Sun, D.L., and Zhenxin Wang, *Functional Gold Nanoparticle-Peptide Complexes as Cell-Targeting Agents.* American Chemical Society, 2008: p. 10293-10297.

[37] Krause, W., *Delivery of diagnostic agents in computed tomography.* Advanced Drug Delivery Reviews, 1999: p. 159 –173.

[38] Xu, C., G.A. Tung, and S. Sun, *Size and Concentration Effect of Gold Nanoparticles on X-ray Attenuation As Measured on Computed Tomography.* Chem Mater, 2008. **20**(13): p. 4167-4169.

[39] Dongkyu Kim, S.P., Jae Hyuk Lee, Yong Yeon Jeong, and Sangyong Jon, *Antibiofouling Polymer-Coated Gold Nanoparticles as a Contrast Agent for in Vivo X-ray Computed Tomography Imaging.* J. AM. CHEM. SOC., 2007. **129**: p. 7661-7665.

[40] Zhang, Y., et al., *Gold nanorods for fluorescence lifetime imaging in biology.* J Biomed Opt, 2010. **15**(2): p. 020504.

[41] Mecker, L.C., et al., *Selective melamine detection in multiple sample matrices with a portable Raman instrument using surface enhanced Raman spectroscopy-active gold nanoparticles.* Anal Chim Acta, 2012. **733**: p. 48-55.

[42] Allen, T.M. and P.R. Cullis, *Drug delivery systems: entering the mainstream.* Science, 2004. **303**(5665): p. 1818-22.

[43] Huang, Y., et al., *Co-administration of protein drugs with gold nanoparticles to enable percutaneous delivery.* Biomaterials, 2010. **31**(34): p. 9086-91.

[44] Mustafa S. Yavuz, Y.C., Jingyi Chen, Claire M. Cobley, Qiang Zhang, MatthewRycenga, Jingwei Xie, Chulhong Kim, Kwang H. Song, Andrea G. Schwartz, Lihong V.Wang and Younan Xia, *Gold nanocages covered by smart polymers for controlled release with near-infrared light.* Nature, 2009. **8**.

[45] Antonin de Fougerolles, H.-P.V., John Maraganore and Judy Lieberman, *Interfering with disease: a progress report on siRNA-based therapeutics.* Nat. Rev. Drug Discov, 2007. **6**: p. 443-453.

[46] Joao Conde, A.A., Vanesa Sanz, Yulan Hernandez, Valentina Marchesano, Furong Tian, Hannah Child, M. Ricardo Ibarra, Pedro V. Baptista, Claudia Tortiglione, and Jesus M. de la Fuente, *Design of Multifunctional Gold Nanoparticles for In Vitro and In Vivo Gene Silencing.* ACSNano, 2012. **6**: p. 8316–8324 ’.

[47] Giljohann, D.A., et al., *Gene Regulation with Polyvalent siRNA−Nanoparticle Conjugates.* Journal of the American Chemical Society, 2009. **131**(6): p. 2072-2073.

[48] Jae-Seung Lee, J.J.G., Kevin T. Love ,Joel Sunshine, Robert Langer, and Daniel G. Anderson*, *Gold, Poly(.-amino ester) Nanoparticles for Small Interfering RNA Delivery*. Nano Lett, 2009. **9**: p. 2402-2406.

[49] Song, W.J., et al., *Gold nanoparticles capped with polyethyleneimine for enhanced siRNA delivery.* Small, 2010. **6**(2): p. 239-46.

[50] Christopher Loo, A.L., Naomi Halas, Jennifer West, and Rebekah Drezek, *Immunotargeted Nanoshells for Integrated Cancer Imaging and Therapy.* Nano Lett, 2005. **5**: p. 709-711.

[51] Wang, J., et al., *Selective photothermal therapy for breast cancer with targeting peptide modified gold nanorods.* Dalton Trans, 2012. **41**(36): p. 11134-44.

[52] El-Sayed, M.A.M.a.M.A., *Comparative Study of the Assemblies and the Resulting Plasmon Fields of Langmuir-Blodgett Assembled Monolayers of Silver Nanocubes and Gold Nanocages.* J. Phys. Chem., 2008. **112**: p. 14618-14625.

[53] Mahmoud, M.A., P. Szymanski, and M.A. El-Sayed, *Different Methods of Increasing the Mechanical Strength of Gold Nanocages.* The Journal of Physical Chemistry Letters, 2012. **3**(23): p. 3527-3531.

[54] Xiaohua Huang, I.H.E.-S., Wei Qian, and Mostafa A. El-Sayed, *Cancer Cell Imaging and Photothermal Therapy in the Near-Infrared Region by Using Gold Nanorods.* J. AM. CHEM. SOC., 2006. **128**: p. 2115-2120.

[55] Xiaohua Huang, X.P., Yiqing Wang,Yuxiang Wang,Dong M. Shin,Mostafa A. El-Sayed, and Shuming Nie, *A Reexamination of Active and Passive Tumor Targeting by Using Rod-Shaped Gold Nanocrystals and Covalently Conjugated Peptide Ligands.* 2010. **4**: p. 5887-5896.

[56] Draz, M.S., et al., *Nanoparticle-mediated systemic delivery of siRNA for treatment of cancers and viral infections.* Theranostics, 2014. **4**(9): p. 872-92.

[57] llkka M. Helander, H.-L.A., KyOsti Latva-Kala and Pertti Koski, *Polyethyleneimine is an effective permeabilizer of Gram-negative bacteria.* Microbiology, 1997. **143**: p. 3 1 93-3 1 99

[58] Geeta Sehgal, J.H., Eric J. Bernhard, Inder Sehgal, Timothy C. Thompson, and Ruth J. Muschel, *Requirement for Matrix Metalloproteinase-9 (Gelatinase B) Expression in Metastasis by Murine Prostate Carcinoma.* American Journal of Pathology, 1998. **152**: p. 591-596.